Amphiphilic Perylene-Calix[4]arene-Hybrids: Synthesis and Tunable Self-Assembly

Fabian Rodler[a], Boris Schade[b], Christof Jäger[c, d,], Susanne Backes[a], Frank Hampel[a],

Christoph Böttcher[b], Timothy Clark[d], and Andreas Hirsch[a]

[a] Department of Chemistry and Pharmacy &
Interdisciplinary Center for Molecular Materials (ICMM),
Friedrich-Alexander-Universität Erlangen-Nürnberg,
Henkestr. 42, 91054 Erlangen, Germany

[b] Forschungszentrum für Elektronenmikroskopie,
Institut für Chemie und Biochemie,
Freie Universität Berlin,
Fabeckstr. 36a, 14195 Berlin, Germany

[c] Department of Chemical and Environmental Engineering,
University of Nottingham,
University Park, Nottingham NG7 2RD, United Kingdom

[d] Computer-Chemie-Centrum & Interdisciplinary Center of Molecular Materials (ICMM),
Friedrich-Alexander-University of Erlangen-Nuremberg,
Nägelsbachstrasse 25, 91052 Erlangen, Germany

Corresponding authors
E-mail: andreas.hirsch@chemie.uni-erlangen.de, christoph.boettcher@fzem.fu-berlin.de

Table of Contents

I. Syntheses S3

a. General Information S3

b. Synthetic procedures S3

Dibutanoic acid methylester-calix[4]arene 5 ..... S3

Calix[4]arene-diacid 6 ..... S5

Dinitro-calix[4]arene 7 ..... S7

Bis-dendro-dinitrocalix[4]arene 8 ..... S9

Bis-dendro-diaminocalix[4]arene 9 ..... S11

Bis-peryleno-bis-dendro-calix[4]arene 10 ..... S13

Bis peryleno-bis-dendro-calix[4]arene (PDC, 3) S15

Preparation of the octa Na- and K-salt of PDC S17

II. Additional UV/Vis- and Fluorescence data S18

a. Concentration dependent absorption of PDC in water S18

b. Fluorescence of PDC in binary water/THF mixtures S18

c. Temperature dependent absorption of PDC in water S19

III. Electron microscopy S20

a. Cryo-TEM Sample Preparation S20

b. Image analysis and processing of 1 mM samples of PDC in binary water/THF mixture S20

c. Crystallisation of PDC from water/THF S23

IV. Molecular Modelling S24

a. MD simulation S29

b. Umbrella Sampling S29

V. Crystallogarphic Data of Dibutanoic acid methylester-calix[4]arene 5 ..... S30

a. General Procedure S30

b. Crystallographic Data S30

I. Syntheses

a. General Information

All solvents and reagents were used as obtained from either *Sigma Aldrich*, *Acors Organics* or *Alfa Aesar*. Reactions were monitored by TLC on silica gel plates (*Merck TLC Silica Gel 60 F_{254} Aluminium plates*). Visualization of the spots was carried out by fluorescence quenching with 254 nm UV light. The recorded NMR-spectra were performed with *BRUKER Avance 300, BRUKER Avance 400* and *JEOL EX 400* spectrometer at room temperature. The ^{1}H-NMR spectra were recorded at 300 MHz or 400 MHz, the ^{13}C-NMR spectra at 75 MHz or 100 MHz. The chemical shifts are relative to the signal of the used solvents $CDCl_3$ (δ_{1H} = 7.26, δ_{13C} = 77.16), CD_2Cl_2 (δ_{1H} = 5.32, δ_{13C} = 53.84) and DMSO-d_6 (δ_{1H} = 2.50, δ_{13C} = 39.52). The appearing coupling constants are given in Hertz. The description of the fine structure means: s = singlet, br.s = broad singlet, d = doublet, m = multiplet. All IR spectra were recorded on a *BRUKER Tensor 27* FT/IR-spectrometer. The displayed maxima are classified in three intensities: s (strong), m (middle), w (weak), br (broad peak) and reported in cm^{-1}. All mass spectra were measured with a *SHIMADZU AXIMA Confidence MALDI-TOF* mass-spectrometer and a *BRUKER maXis 4G ESI-UHR-TOF* mass spectrometer. The elemental analyses were performed on a *CE INSTRUMENTS EA 1110 CHNS* and a *EURO VECTOR Euro EA3000.* The UV/Vis-spectra were measured on a *VARIAN Cary 5000 UV/Vis-nIR* spectrometer and all fluorescence spectra on a *SHIMADZU RF-5301 PC* spectrometer.

b. Synthetic procedures

Dibutanoic acid methylester-calix[4]arene 5

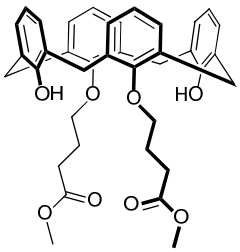

A suspension of calix[4]arene[1] **4** (1.81 g, 4.26 mmol, 1.0 eq), K_2CO_3 (1.18 g, 8.53 mmol, 2.0 eq) and Bromide (2.16, 3.10 g, 17.1 mmol, 4.0 eq) in dry MeCN (25 ml) was stirred 12 h at 80°C. The solvent was removed under reduced pressure and CH_2Cl_2 (100 ml) was added. The organic layer was washed with water (2x), 1M HCl (2x 10 ml), water (20 ml) and brine. The organic layer was separated, dried with $MgSO_4$, filtered and the solvent was removed under reduced pressure. The residue was recrystallized from CH_2Cl_2/MeOH to afford white crystals. Yield 2.05 g (77%)

^{1}H-NMR (400 MHz, $CDCl_3$) δ 8.04 (s, 2 H, O*H*), 7.04 (d, 4 H, ^{3}J = 8.0 Hz, C*H*), 6.89 (d, 4 H, ^{3}J = 8.0 Hz, C*H*), 6.73 (t, 2 H, ^{3}J = 8.0 Hz, C*H*), 6.64 (t, 2 H, ^{3}J = 8.0 Hz, C*H*), 4.24 (d, 4 H, ^{2}J = 12.2 Hz, CH_2), 4.05 (t, 4 H, ^{3}J = 6.0 Hz, CH_2), 3.70 (s, 6 H, CH_3), 3.97 (d, 4 H, ^{2}J = 12.2 Hz, CH_2), 2.90 (t, 4 H, ^{3}J = 6.1 Hz, CH_2), 2.31-2.37 (m, 4 H, CH_2);

^{13}C-NMR (100 MHz, $CDCl_3$) δ 173.7, 153.3, 151.5, 133.3, 129.0, 128.5, 128.0, 125.5, 119.1, 75.3, 51.6, 31.4, 30.5, 25.5. **FT-IR** $\tilde{\nu}$ (ATR) [cm^{-1}] = 3319 [br], 2917 [w], 2872 [w], 1752 [s], 1466 [m], 1440 [m], 1353 [m], 1259 [m], 1235 [m], 1156 [s], 1036 [s], 764 [s], 754 [s]. **MALDI-TOF MS** (matrix: sin, CH_2Cl_2): *m/z* = 647 [M + Na]$^+$. **EA**: $C_{38}H_{40}O_8$ x MeOH, calculated: C 71.62, H 6.91, found: C 71.67, H 6.63.

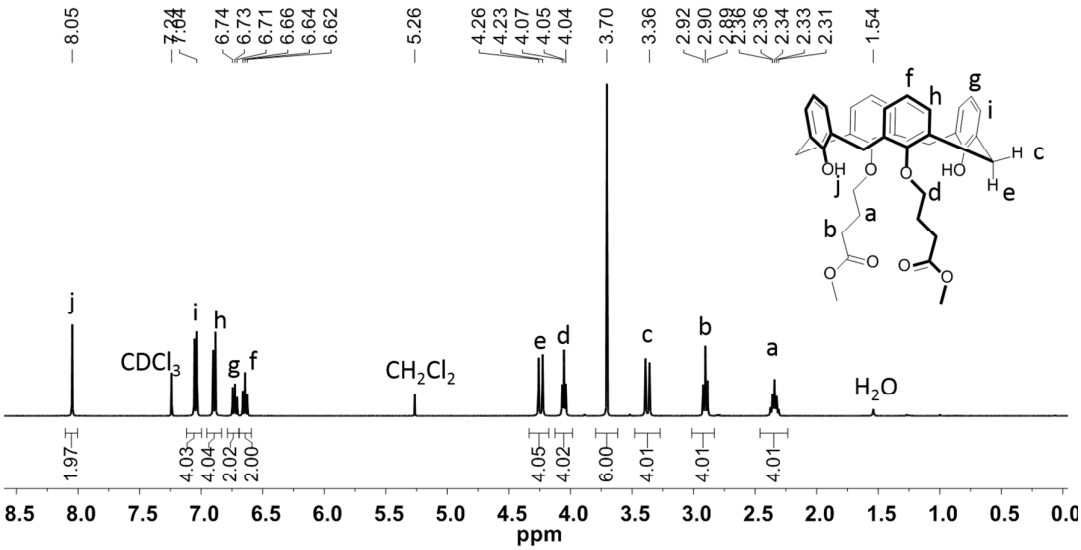

Figure SI 1: ^{1}H-NMR spectrum of compound **5** in $CDCl_3$ (400 MHz).

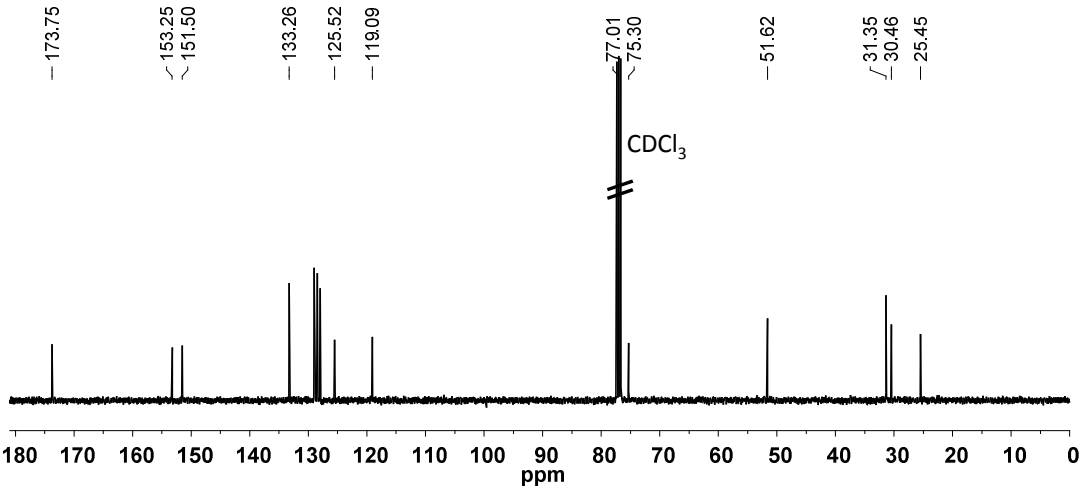

Figure SI 2: ^{13}C-NMR spectrum of compound **5** in $CDCl_3$ (100 MHz).

Calix[4]arene-diacid 6

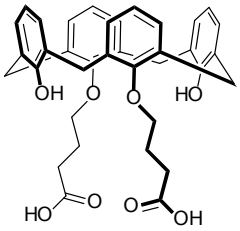

Calix[4]arene dimethylester **5** (10.0 g, 16.0 mmol, 1.0 eq) was suspended in acetone (300 ml) and potassium hydroxide (17.9 g, 320 mmol, 20 eq) was added. The brownish suspension was stirred 48 h at room temperature. The solvent was removed under reduced pressure and water was added (150 ml). The mixture was poured into 4N HCl (150 ml) and the suspension was stirred 5 min at room temperature. The precipitate was filtered and washed with water. The solid was suspended in DCM (200 ml) and stirred for 5 min at room temperature. The white precipitate was filtered and washed with DCM. The pure product was dried in vacuum. Yield 9.24 g (97 %)

^{1}H-NMR (400 MHz, DMSO-d_6) δ 12.19 (s, 2 H, COO*H*), 8.47 (s, 2H, O*H*), *7*.15 (d, 4 H, ^3J = 6.0 Hz, C*H*), 7.05 (d, 4 H, ^3J = 8.8 Hz, C*H*), 6.79 (t, 2 H, ^3J = 6.0 Hz, C*H*), 6.59 (t, 2 H, ^3J = 8.8 Hz, C*H*), 4.17 (d, 4 H,^2J = 12.1 Hz, CH_2), 4.01 (t, 4 H, ^3J = 6.4 Hz, CH_2), 3.45 (d, 4 H, ^2J = 12.1 Hz, CH_2), 2.80 (t, 4 H, ^3J = 6.7 Hz, CH_2), 2.18-2.25 (m, 4 H, CH_2). **^{13}C-NMR** (100 MHz, DMSO-d_6) δ 174.4, 152.6, 151.4, 133.8, 128.9, 128.6, 127.8, 125.4, 119.2, 75.4, 30.5, 29.9, 25.1. **FT-IR** $\tilde{\nu}$ (ATR) [cm^{-1}] 3348 [br], 3027 [w], 2888 [w], 1657 [w], 1468 [m], 1455 [m], 1245 [m], 1203 [m], 1090 [s], 932 [s], 744 [s]. **MALDI-TOF MS** (matrix: without matrix, THF): *m/z* = 619 [M + Na]$^+$, *m/z* = 635 [M + K]$^+$. **EA:** $C_{36}H_{36}O_8$, calculated: C 72.47, H 6.08, found: C 72.02, H 6.15.

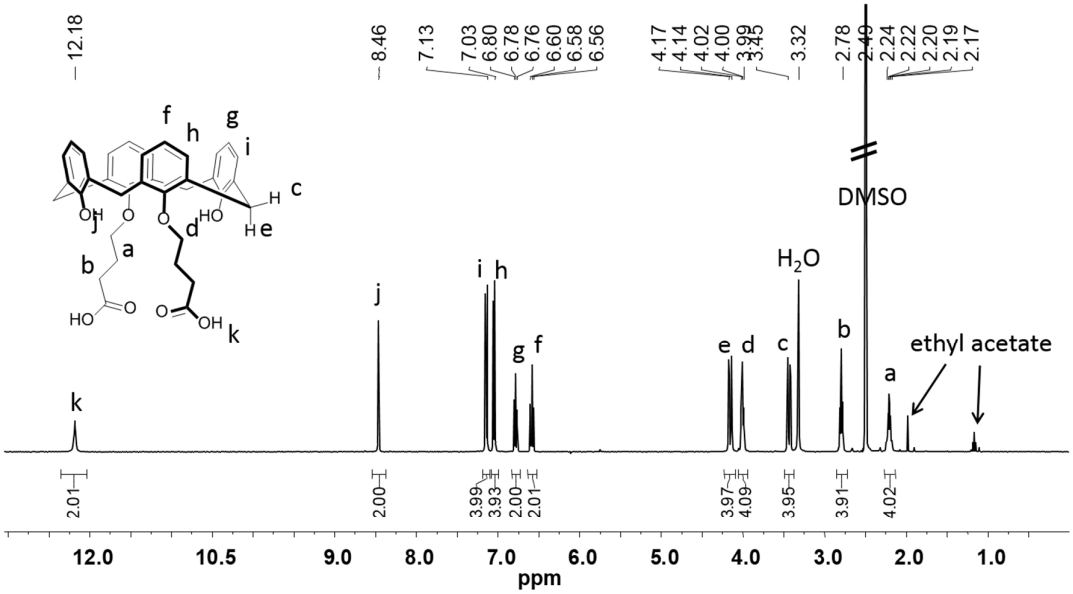

Figure SI 3: ^{1}H-NMR spectrum of compound **6** in DMSO-d_6 (400 MHz).

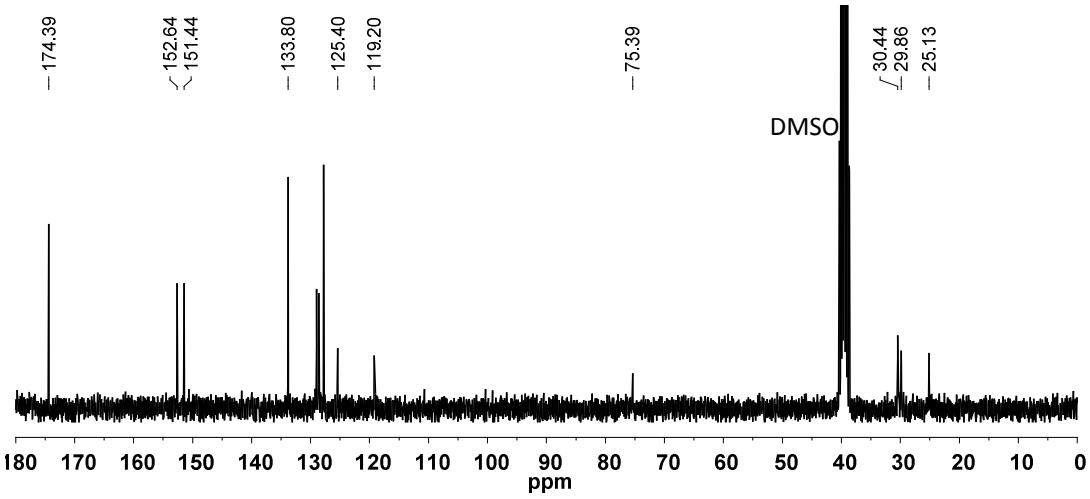

Figure SI 4: ^{13}C-NMR spectrum of compound **6** in DMSO-d_6 (75 MHz).

Dinitro-calix[4]arene 7

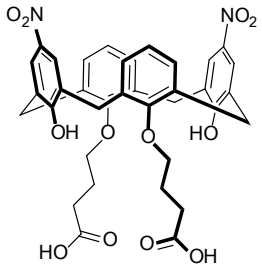

To a solution of compound **6** (0.50 g, 0.84 mmol, 1.0 eq) and glacial acetic acid (1.73 ml, 30.2 mmol, 36.0 eq) in DCM (13 ml) was added 65% HNO_3 (2.86 ml) at 0°C. The reaction mixture was stirred at this temperature for 15 min, where upon water (40 ml) was added. The slight yellow precipitate was filtered and washed with water (3 x 20 ml) and DCM (3 x 20 ml). The solid product was dried in vacuum. Yield: 0.36 g (62 %)

^{1}H-NMR (300 MHz, DMSO-d_6) δ 12.23 (br.s, 2 H, COO*H*), 9.64 (s, 2H, O*H*), 8.28 (s, 4 H, C*H*), 7.18 (d, 4 H, ^3J = 9.0 Hz, C*H*), 6.87 (t, 2 H, ^3J = 9.0 Hz, C*H*), 4.15 (d, 4 H, ^2J = 12.0 Hz, CH_2), 4.06 (t, 4 H, ^3J = 6.0 Hz, CH_2), 3.77 (d, 4 H, ^2J = 12.0 Hz, CH_2), 2.75 (t, 4 H, ^3J = 6.0 Hz, CH_2), 2.20-2.27 (m, 4 H, CH_2). **^{13}C-NMR** (75 MHz, $CDCl_3$) δ 174.2, 159.3, 151.4, 139.5, 132.4, 129.7, 128.7, 126.0, 124.6, 75.7, 30.7, 29.8, 25.0. **FT-IR** $\tilde{\nu}$ (ATR) [cm^{-1}] 3187 [br], 2926 [w], 1712 [s], 1594 [w], 1339 [s], 1110 [w], 1075 [m], 1030 [m], 941 [m], 766 [m]. **MALDI-TOF MS** (matrix: dhb, THF): *m*/*z* = 709 [M + Na]$^+$.

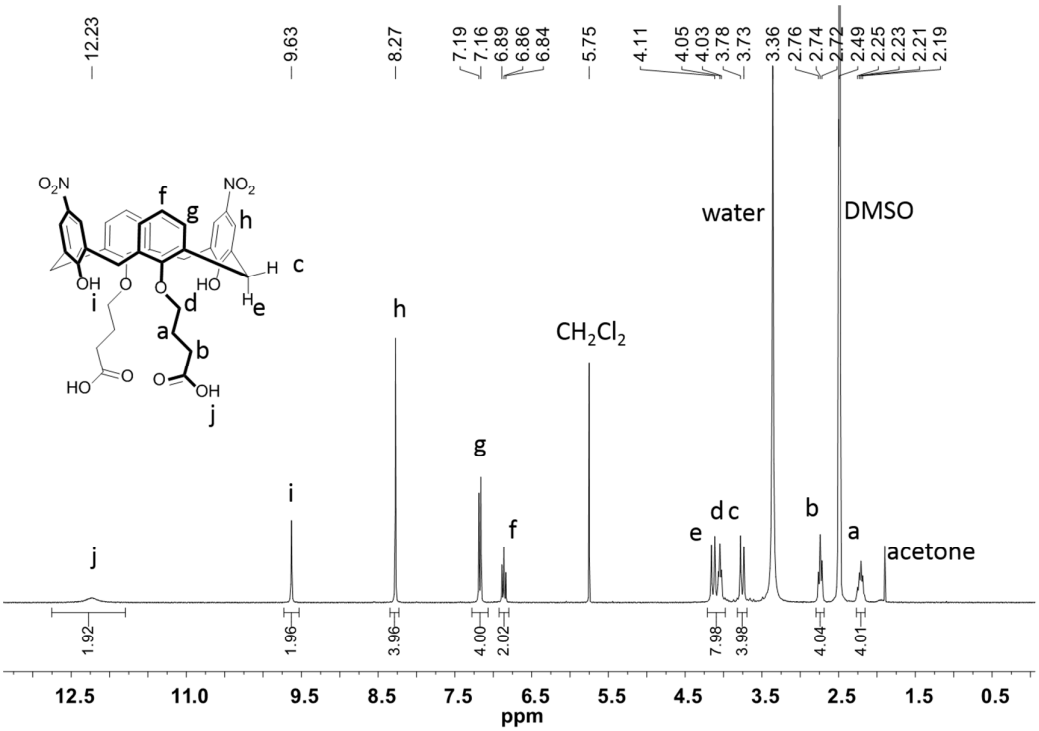

Figure SI 5: ^{1}H-NMR spectrum of compound **7** in DMSO-d_6 (300 MHz).

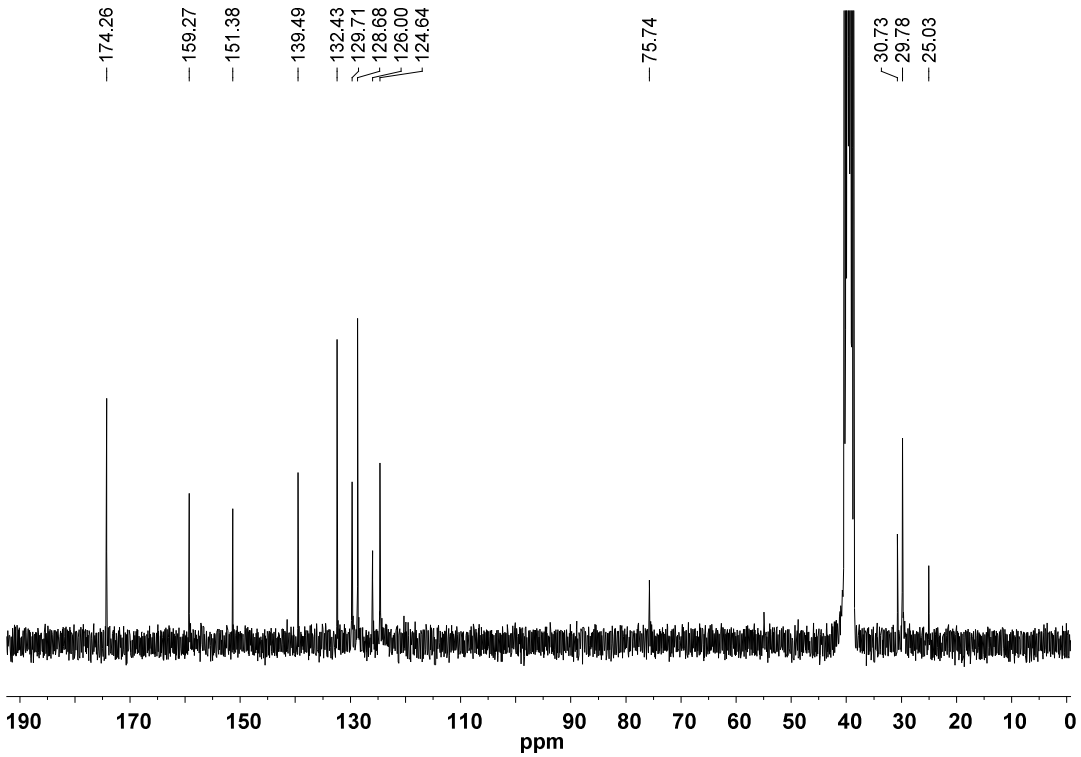

Figure SI 6: ^{13}C-NMR spectrum of compound **7** in DMSO-d_6 (75 MHz).

Bis-dendro-dinitrocalix[4]arene 8

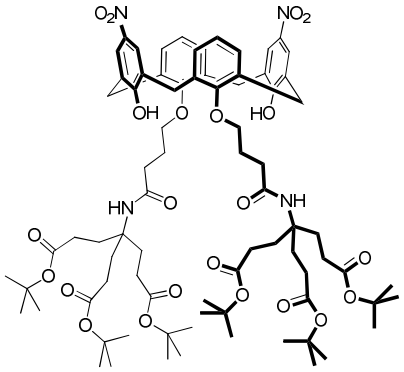

To a solution of compound **7** (1.37 g, 2.00 mmol, 1.0 eq) and Newkome-dendrimer **11** (4.99 g, 12.0 mmol, 6.0 eq) in dry THF (15 ml) was added DMT-MM (1.44 g, 5.20 mmol, 2.6 eq) and the resulting suspension was stirred for 2 days at room temperature. The solvent was removed under reduced pressure, the residue was dissolved in DCM (20 ml) and washed with water (2 x 20 ml), saturated aqueous $NaHCO_3$-solution (2 x 20 ml) and brine (20 ml). The organic layer was separated and dried with $MgSO_4$. The drying agent was removed by filtration and the solvent was removed under reduced pressure. The residue was purified by column chromatography (R_f: 0.78, SiO_2, DCM/ethyl acetate = 7/1) and the solvent was removed under reduced pressure and the colorless solid was dissolved in a small amount of THF and precipitated with an excess of water. Lyophilisation afforded a colorless solid. Yield: 2.26 g (77 %)

^{1}H-NMR (400 MHz, $CDCl_3$) δ 9.31 (s, 2H, O*H*), 8.02 (s, 4 H, C*H*), 6.97 (d, 4 H, ^3J = 9.0 Hz, C*H*), 6.83 (t, 2 H, ^3J = 9.0 Hz, C*H*), 6.58 (s, 2 H, N*H*), 4.26 (d, 4 H, ^2J = 12.0 Hz, CH_2), 4.12 (t, 4 H, ^3J = 6.0 Hz, CH_2), 3.51 (d, 4 H, ^2J = 12.0 Hz, CH_2), 2.65 (t, 4 H, ^3J = 6.0 Hz, CH_2), 2.30-2.37 (m, 4 H, CH_2), 2.18-2.22 (m, 12 H CH_2-dendrimer), 1.95-1.98 (m, CH_2-dendrimer), 1.39 (s, 54 H, CH_3-^{t}Bu). **^{13}C-NMR** (100 MHz, $CDCl_3$) δ 172.8, 171.6, 159.4, 151.5, 139.9, 131.8, 129.7, 128.4, 126.0, 124.6, 80.6, 76.0, 57.5, 32.3, 31.3, 30.0, 29.8, 28.1, 26.0. **FT-IR** $\tilde{\nu}$ (ATR) [cm^{-1}] 3178 [br], 2978 [w], 1712 [s], 1661 [w], 1590 [w], 1365 [w], 1261 [s], 1213 [m], 1148 [s], 1100 [m], 847 [w]. **MALDI-TOF MS** (matrix: sin, CH_2Cl_2): *m/z* = 1504 $[M + Na]^+$, 1520 $[M + K]^+$.

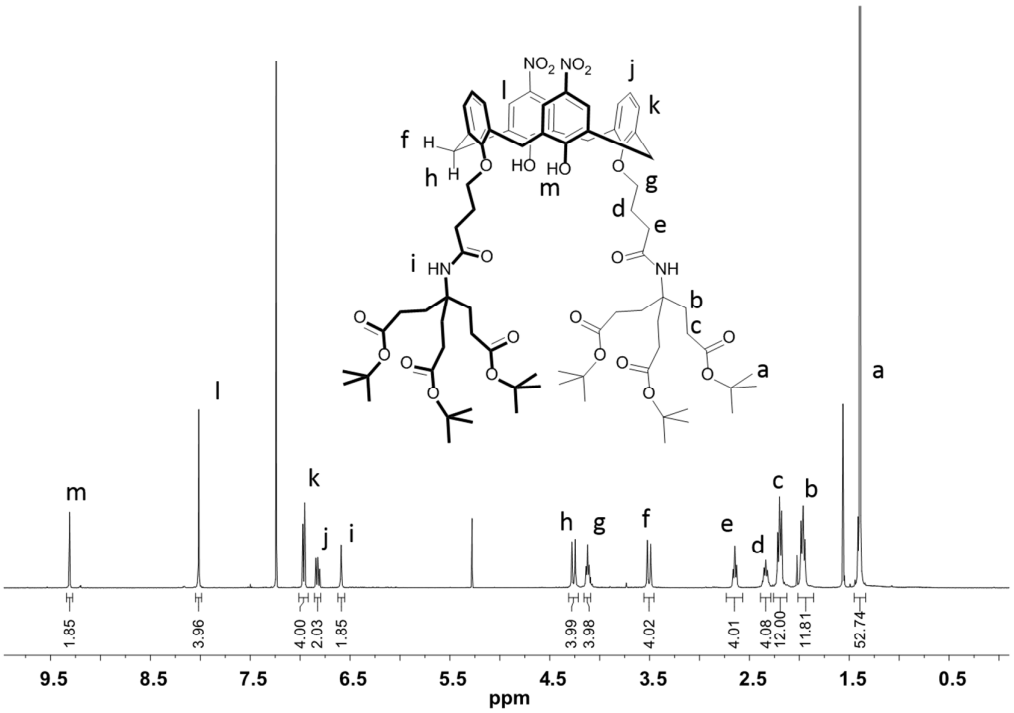

Figure SI 7: ^{1}H-NMR spectrum of compound **8** in $CDCl_3$ (400 MHz).

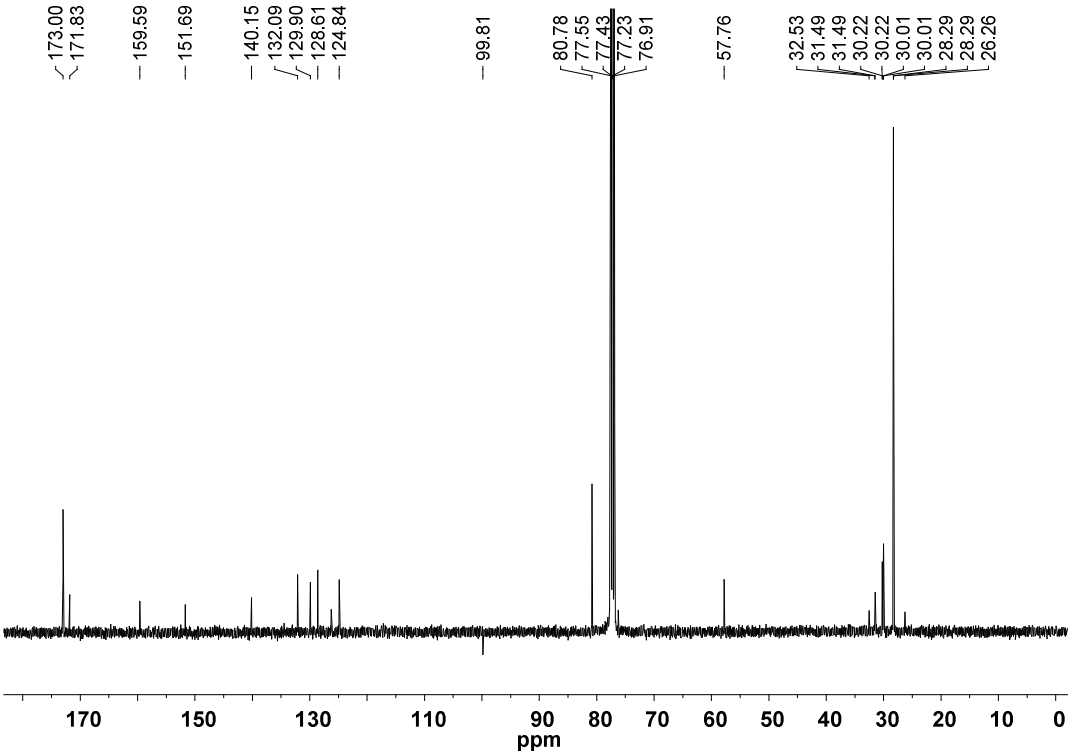

Figure SI 8: ^{13}C-NMR spectrum of compound **8** in $CDCl_3$ (100 MHz).

Bis-dendro-diaminocalix[4]arene 9

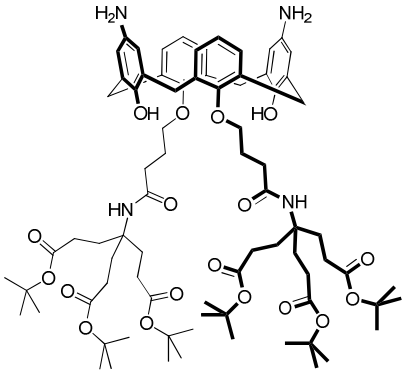

To a suspension of dinitro-precursor **8** (660 mg, 0.445 mmol, 1.0 eq) in dry EtOH (30 ml) was added catalytic amounts of palladium on activated charcoal and hydrazine monohydrate (0.22 ml, 223 mg, 4.45 mmol, 10.0 eq) under N_2-atmosphere and the mixture was heated at reflux (80 °C) for 4 hours. After cooling to room temperature, the mixture was filtered over a celite pad and the mixture was concentrated under reduced pressure until a precipitate was formed. For complete crystallization, the dispersion was cooled in a refrigerator for 12 hours. The precipitate was filtered, washed with cold ethanol and dried *in vacuo* to afford a colorless solid. Yield: 631 mg (100 %)

^{1}H-NMR (300 MHz, $CDCl_3$) δ 7.60 (s, 2H, O*H*), 6.89 (d, 4 H, ^3J = 9.0 Hz, C*H*), 6.72 (t, 2 H, ^3J = 9.0 Hz, C*H*), 6.41 (s, 4 H, C*H*), 6.37 (s, 2 H, N*H*), 4.20 (d, 4 H, ^2J = 12.0 Hz, CH_2), 4.01 (t, 4 H, ^3J = 6.0 Hz, CH_2), 3.24 (d, 4 H, ^2J = 12.0 Hz, CH_2), 2.69 (t, 4 H, ^3J = 6.0 Hz, CH_2), 2.26-2.30 (m, 4 H, CH_2), 2.15-2.20 (m, 12 H CH_2-dendrimer), 1.90-1.95 (m, CH_2-dendrimer), 1.40 (s, 54 H, CH_3-^{t}Bu). **^{13}C-NMR** (75 MHz, $CDCl_3$) δ 172.7, 171.9, 151.6, 145.4, 138.5, 133.5, 129.0, 119.2, 118.8, 115.9, 80.4, 77.3, 57.4, 31.5, 30.0, 29.8, 28.3, 28.1, 28.0. **FT-IR** $\tilde{\nu}$ (ATR) [cm^{-1}] 3348 [br], 2975 [w], 2934 [w], 1725 [s], 1654 [w], 1539 [w], 1483 [m], 1456 [m], 1366 [m], 1247 [w], 1149 [s], 847 [m], 760 [m]. **MALDI-TOF MS** (matrix: sin, CH_2Cl_2): *m/z* = 1444 $[M + Na]^+$, 1460 $[M + K]^+$.

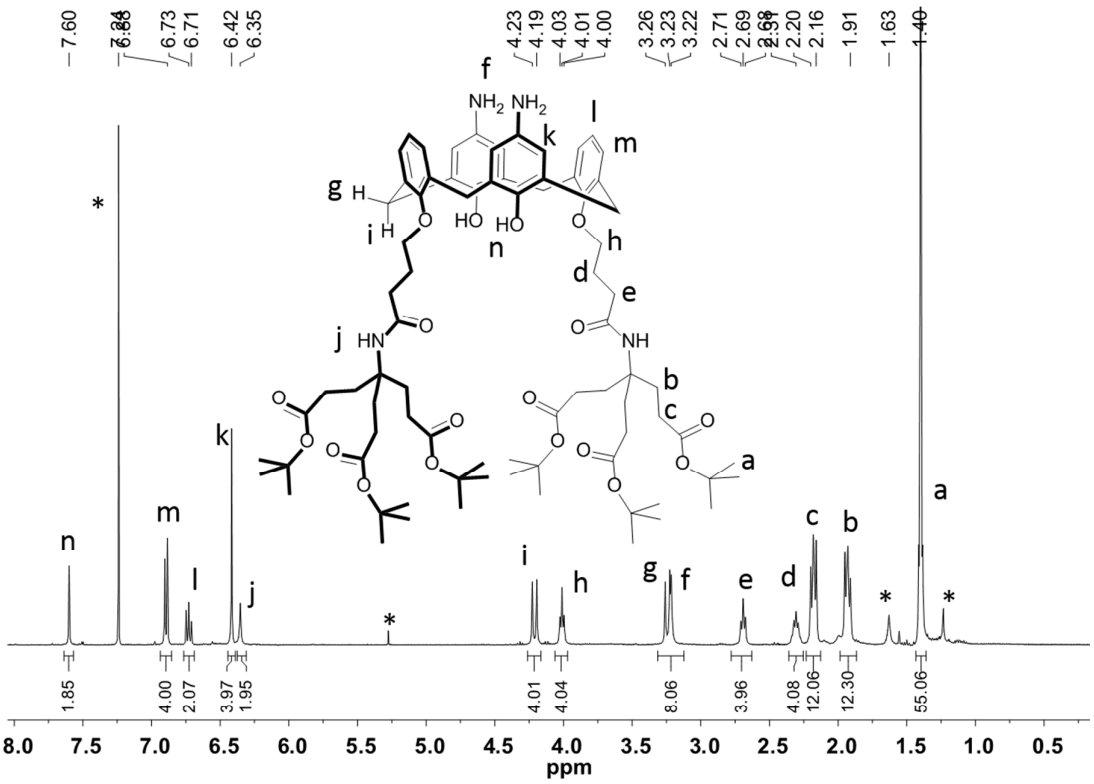

Figure SI 9: ^{1}H-NMR spectrum of compound **9** in $CDCl_3$ (400 MHz).

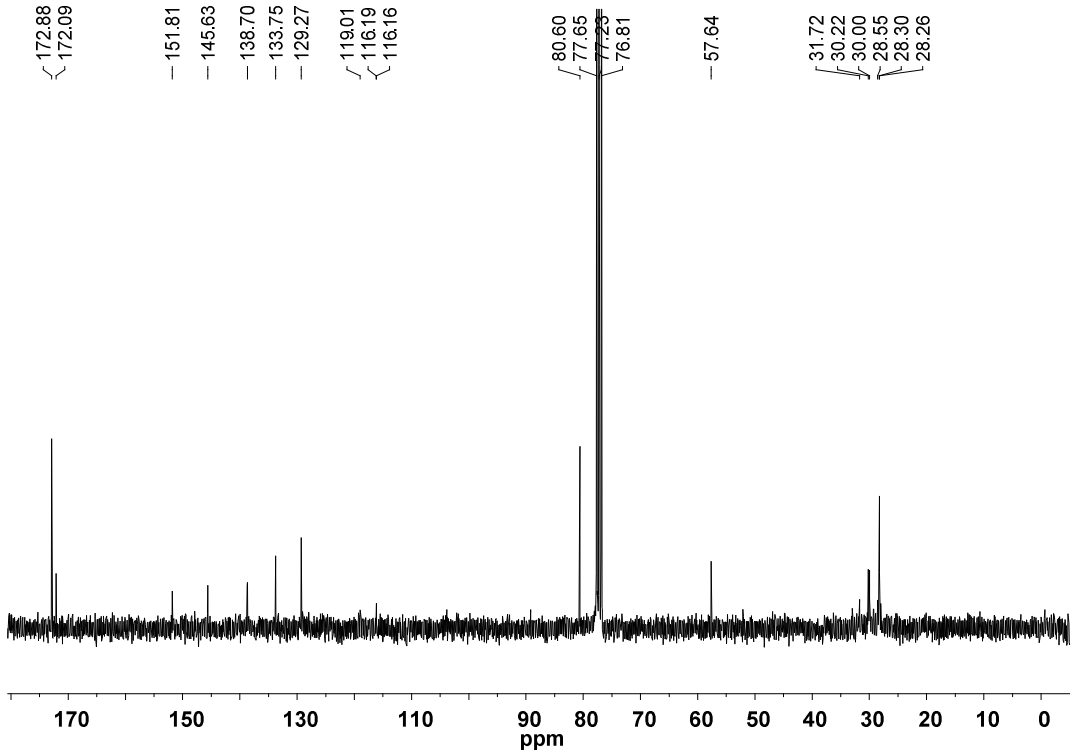

Figure SI 10: ^{13}C-NMR spectrum of compound **9** in $CDCl_3$ (100 MHz).

Bis-peryleno-bis-dendro-calix[4]arene 10

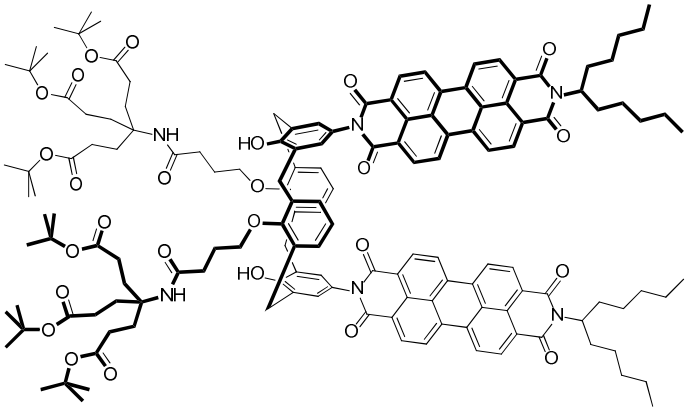

Under N_2-atmosphere, a suspension of diaminocalix[4]arene **9** (192 mg, 0.135 mmol, 1.0 eq), perylene-mono-imid-monoanhydrid **12** (220 mg, 0.41 mmol, 3.0 eq) and anhydrous zinc acetate (99.1 mg, 0.54 mmol, 4.0 eq) in quinolone (2 ml) was stirred for 2 hours at 120 °C. The mixture was allowed to cool to room temperature and the residue was dissolved in DCM (20 ml). The organic layer was washed with aqueous citric acid solution (10 %; 3 x 20 ml), water (3 x 20 ml) and brine. The organic layer was separated, dried with anhydrous $MgSO_4$ and the drying agent was removed by filtration. The solvent was evaporated and the residue was purified by column chromatography (R_f: 0.49, SiO_2, DCM/isopropanol = 20/1). The solvent was removed *in vacuo* and the residue was dissolved in a small amount of THF. The product was precipitated by an excess of water and the solvents were removed by lyophilization affording a deep red, crystalline solid. Yield: 166 mg (50 %)

^{1}H-NMR (300 MHz, $CDCl_3$) δ 8.17-8.68 (m, 16 H, C*H* – perylene), 8.09 (s, 2H, O*H*), 7.14 (s, 4 H, C*H*), 6.57 (br.s, 4 H, C*H*), 6.35 (s, 2 H, C*H*), 6.02 (br.s, 2 H, N*H*), 5.17-5.24 (m, 2 H, C*H*), 4.32 (d, 4 H, ^2J = 13.6 Hz, CH_2), 4.02-4.12 (m, 4 H, CH_2), 3.49 (d, 4 H, ^2J = 13.6 Hz, CH_2), 2.71 (t, 4 H, ^3J = 6.4 Hz, CH_2), 2.29-2.38 (m, 4 H, CH_2), 2.24-2.28 (m, 12 H, CH_2-dendrimer), 1.99-2.03 (m, 12 H, CH_2-dendrimer), 1.88-1.92 (m, 4H, CH_2), 1.42 (s, 54 H, CH_3-^{t}Bu), 1.24-1.37 (s, 28 H, CH_2), 0.85 (t, 12 H, ^3J = 6.8 Hz, CH_3). **^{13}C-NMR** (100 MHz, $CDCl_3$) δ 172.9, 171.9, 163.4, 153.9, 151.9, 134.3, 134.2, 131.8, 131.3, 129.4, 129.3, 129.2, 128.6, 126.1, 125.9, 125.3, 123.9, 123.4, 122.9, 80.4, 75.3, 57.6, 54.9, 33.2, 31.8, 31.7, 30.1, 29.9, 28.1, 26.7, 26.2, 22.6, 14.1. **FT-IR** $\tilde{\nu}$ (ATR) [cm^{-1}] 2926 [m], 2856 [w], 1725 [s], 1656 [s], 1594 [m], 1577 [m], 1540 [m], 1481 [w], 1391 [s], 1366 [s], 1344 [s], 1311 [s], 1254 [s], 1130 [s], 989 [w], 849 [m]. **MALDI-TOF MS** (matrix: sin, $CHCl_3$): *m/z* = 2500 [M + Na]$^+$. **EA:** $C_{150}H_{174}N_6O_{26}$ x 5 DCM, calculated: C 64.66, H 6.58, N 2.83; found: C 64.50, H 6.65, N 3.05. **UV/Vis** ($CHCl_3$): λ_{max} [nm] (ε [M^{-1} cm^{-1}]) = 459 (29000), 490 (83000), 527 (138000).

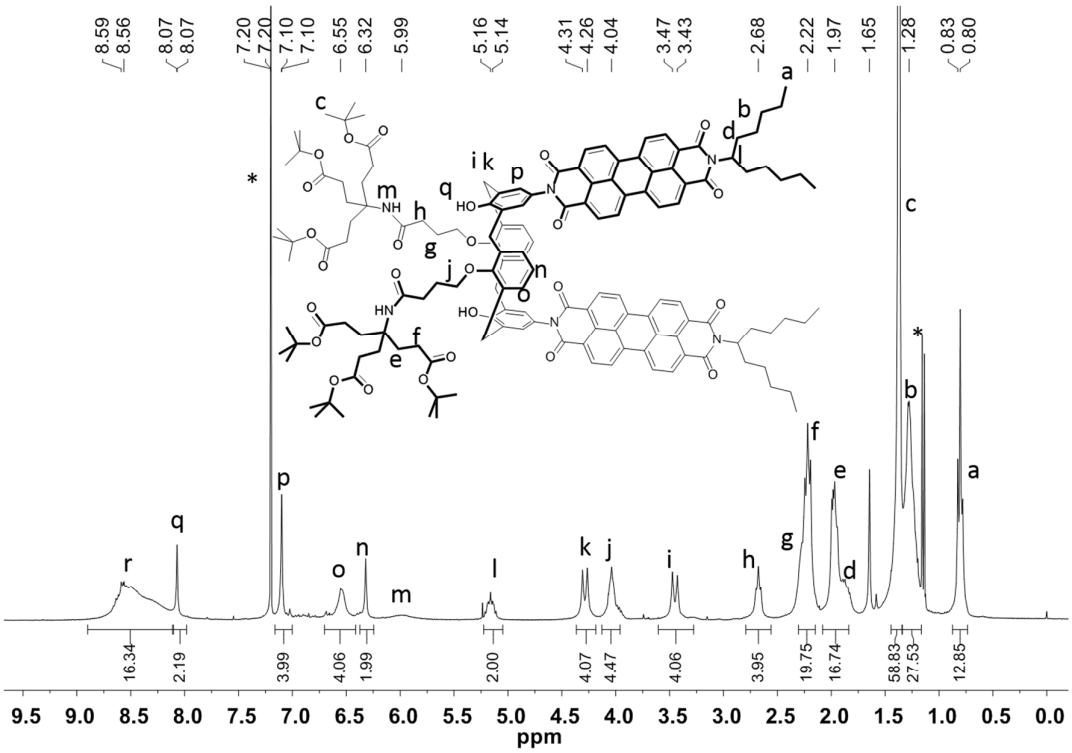

Figure SI 11: ^{1}H-NMR spectrum of compound **10** in $CDCl_3$ (400 MHz).

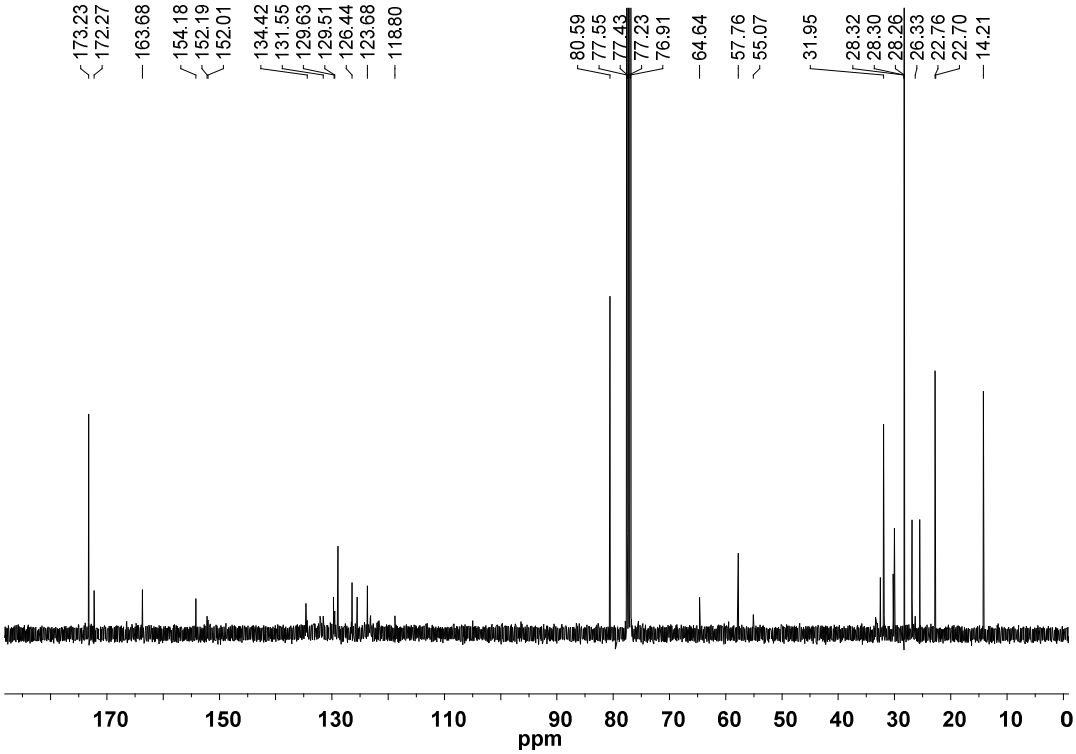

Figure SI 12: ^{13}C-NMR spectrum of compound **10** in $CDCl_3$ (100 MHz).

Bis peryleno-bis-dendro-calix[4]arene (PDC, 3)

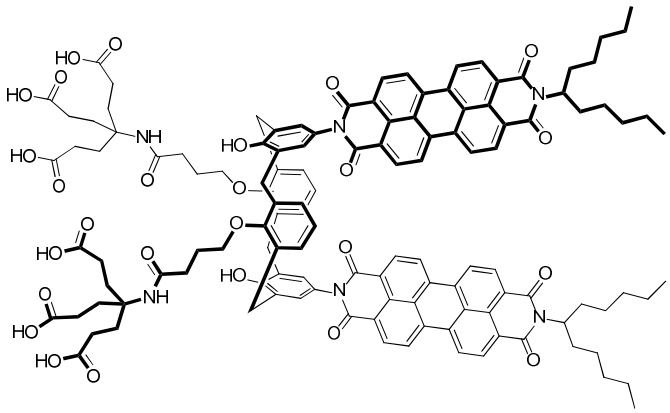

A solution of perylene diimid precursor **10** (106 mg, 0.043 mmol, 1.0 eq) in a mixture of $CHCl_3$ (5 ml) and TFA (5 ml) was stirred for 12 hours at room temperature. The solvent was removed under reduced pressure and the residue was suspended in diethyl ether (10 ml). The suspension was stirred for 1 hour at room temperature. The precipitate was filtered and washed with diethyl ether. The deep red solid was dried *in vacuo*. Yield: 83.8 mg (91 %)

^{1}H-NMR (400 MHz, CD_2Cl_2/TFA-d_1) δ 8.81-8.88 (m, 16 H, C*H* – perylene), 8.61 (br.s, 2H, O*H*), 7.19 (s, 4 H, C*H*), 7.02 (d, 4 H, ^3J = 7.2 Hz, C*H*), 6.90 (t, 2 H, ^3J = 7.2 Hz, C*H*), 5.18-5.27 (m, 2 H, C*H*), 4.31 (d, 4 H, ^2J = 13.2 Hz, CH_2), 4.15-4.23 (m, 4 H, CH_2), 3.60 (d, 4 H, ^2J = 13.2 Hz, CH_2), 2.92 (t, 4 H, ^3J = 6.4 Hz, CH_2), 2.46-2.60 (m, 12 H + 4 H, CH_2-dendrimer + CH_2), 2.18-2.26 (m, 4 H + 12 H, CH_2-dendrimer + CH_2), 1.27-1.39 (s, 24 H, CH_2), 0.85 (t, 12 H, ^3J = 6.8 Hz, CH_3). **^{13}C-NMR** (100 MHz, CD_2Cl_2/TFA-d_1) δ 180.2, 179.3, 166.1, 152.2, 151.2, 136.9, 135.9, 133.8, 130.2, 130.0, 129.4, 129.2, 128,4, 127.2, 126.9, 125.0, 124.8, 123.7, 122.9, 75.3, 59.5, 56.9, 32.8, 32.1, 30.1, 29.2, 28.9, 28.3, 27.0, 23.0, 14.0. **MALDI-TOF MS** (matrix: sin, CD_2Cl_2/TFA-d_1): *m*/*z* = 2164 $[M + Na]^+$, 2181 $[M + K]^+$. **UV/Vis** $[X^{8-} \cdot 8\ Na^+$ (water)]: λ_{max} [nm] (ε $[M^{-1}\ cm^{-1}]$) = 503 (48000), 547 (29000).

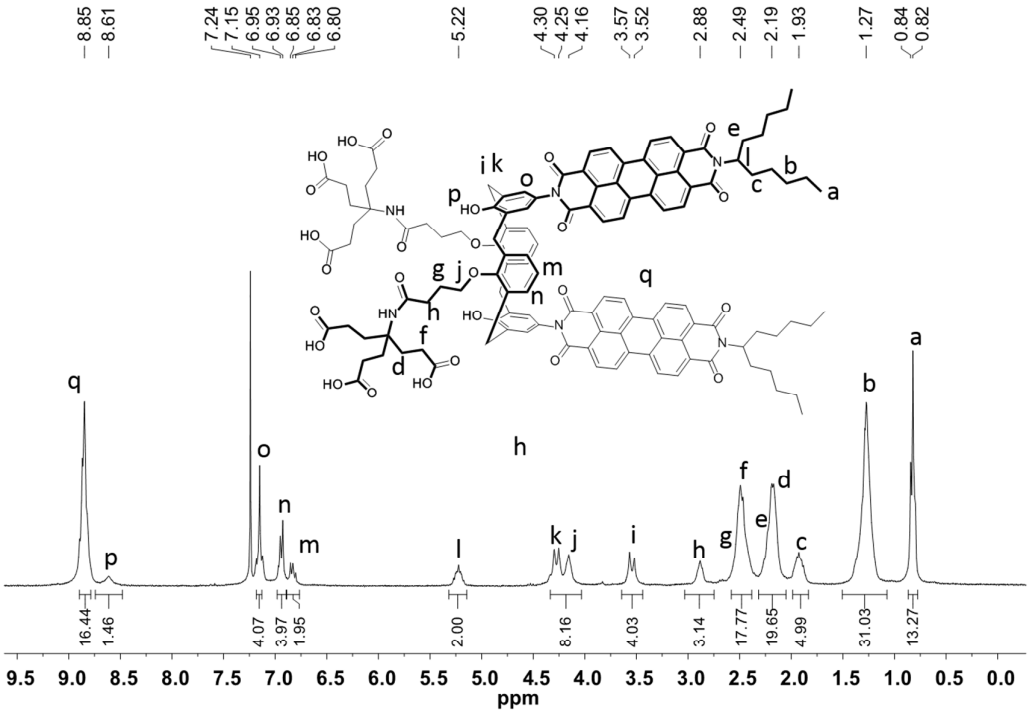

Figure SI 13: 1H-NMR spectrum of **PDC** in CDCl3 + TFA-d1 (400 MHz).

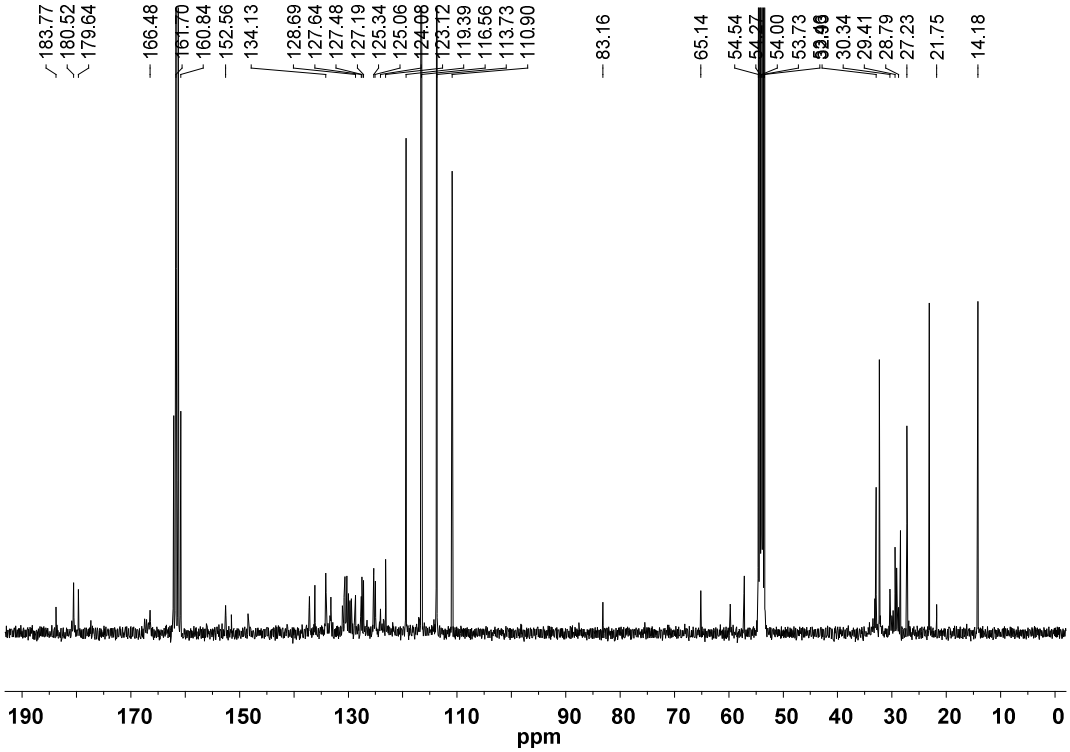

Figure SI 14: ^{13}C-NMR spectrum of **PDC** in CD_2Cl_2 + TFA-d_1 (100 MHz).

Preparation of the octa Na- and K-salt of PDC

PDC (20.0 mg, 0.0093 mmol) was dispersed in water (2 ml) and 8 equivalents of 1 M aqueous NaOH (KOH) – solution were added. The mixture was stirred until a clear solution was formed. The water was removed by lyophilization to afford a deep red powder, which is soluble in pure water and which was used for UV/Vis, fluorescence and cryo-TEM experiments.

II. Additional UV/Vis- and Fluorescence data

a. Concentration dependent absorption of PDC in water

Concentration dependent UV/Vis-spectroscopy in a range between 10^{-2} – 10^{-7} mol L^{-1} showed neither shifts of the absorption maxima nor any change of the signal intensity ratios. The UV/Vis-measurements were performed using a 10^{-2} mol L^{-1} stock solution diluting to the corresponding concentrations.

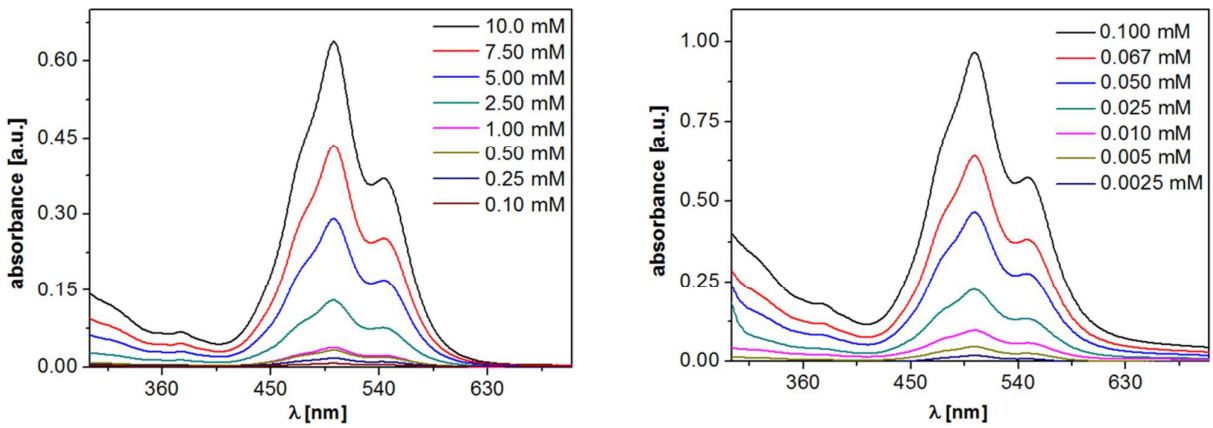

Figure SI 15: Concentration dependent UV/Vis-spectra of **PDC** in water. Note the different concentration ranges between 10^{-2} mol L^{-1} and 10^{-4} mol L^{-1} (left) and between 10^{-4} mol L^{-1} and 2.5 x 10^{-6} mol L^{-1} (right).

b. Fluorescence of PDC in binary water/THF mixtures

The titration of a 0.1 mol L^{-1} aqueous stock solution of **PDC** with different amounts of THF shows a gradual inversion of the band intensities which indicates the transition from aggregated into free perylene diimid moieties, probably in the open conformation, of the **PDC**. The steep increase in emission intensity of the free perylenes at higher THF content illustrates a strong quenching of the fluorescence in PDC aggrgates.

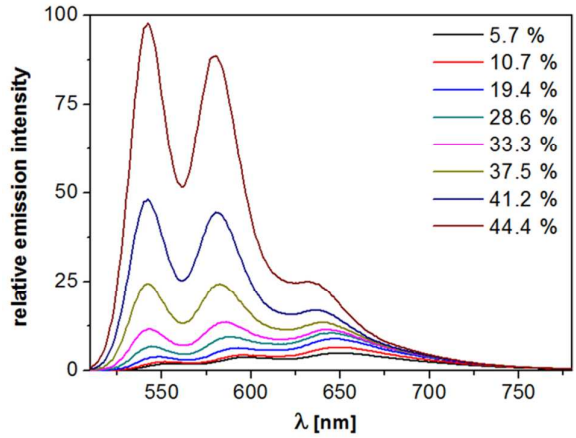

Figure SI 16: Fluorescence spectra of **PDC** in binary water/THF mixtures with different THF contents ranging from 0 - 44% (v/v). Excitation wavelength: 492 nm.

c. Temperature dependent absorption of PDC in water

As was stated in the paper, cryo-TEM measurements revealed that the thermal annealing of the aqueous samples of **PDC** for 5 hours at 85°C did not change the polymorphous appearance of the aggregates. This observation may result from two reasons; either, the polymorphous distribution reflects an equilibrium state of the aggregation process which is resumed upon cooling or the once formed aggregates are stable within this temperature range. To decide between these two possibilities, we performed temperature dependent UV/Vis measurements of a 0.1 mM solution of **PDC** in pure water. The temperature independency of the spectra clearly indicates that the aggregates are thermally stable.

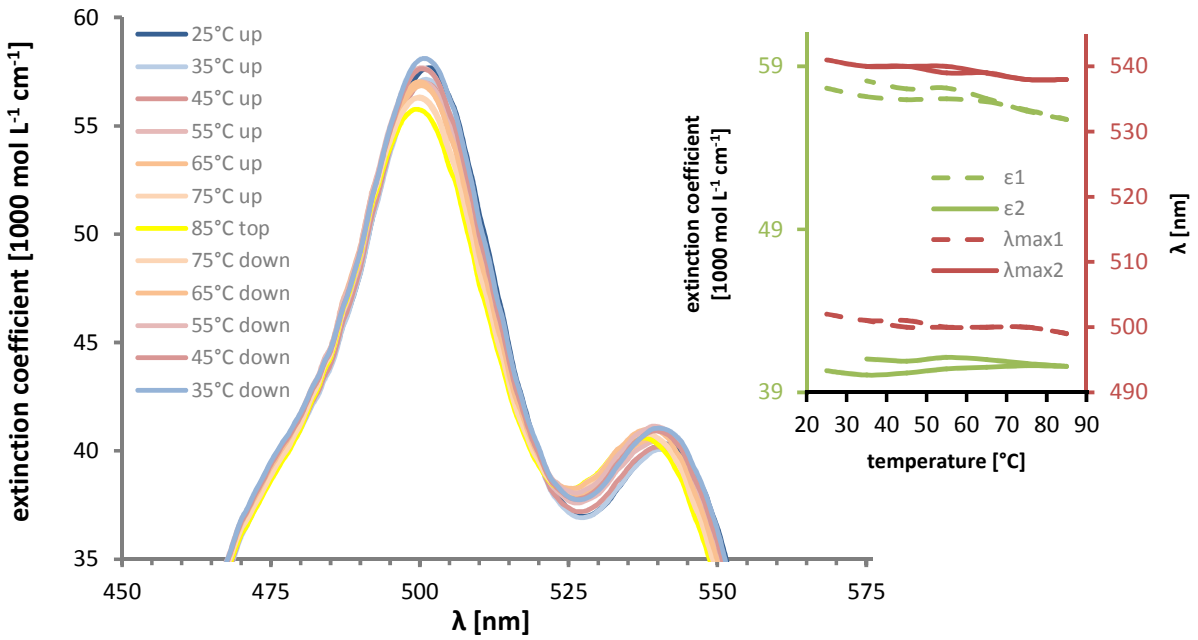

Figure SI 17: Temperature dependence of the UV/Vis spectra of **PDC** in water. The inset displays the course of the extinctin coefficients at λ_{max} (green graph) and the shift of λ_{max} (red graph).

III. Electron microscopy

a. Cryo-TEM Sample Preparation

Samples for cryo-TEM were prepared by placing an aliquot of the sample solution on commercially available holey carbon covered copper grids (R 1/4 batch of Quantifoil Micro Tools GmbH, Jena, Germany). The supernatant fluid was blotted until an ultra-thin film is obtained, which spans the holes of the support film. The grids were immediately vitrified in liquid ethane by the use of a spring-loaded plunging device. The vitrified samples were then transferred into the electron microscope under liquid nitrogen using a Gatan cryo-holder and stage (model 626, Gatan Inc., California, USA). Microscopy was performed at 94 K sample temperature with a Philips CM12 transmission electron microscope (FEI, Oregon, USA) at a primary magnification of 58,300 x (100 kV, LaB_6-illumination). Images were recorded on Kodak® SO-163 negative film and digitized with a Epson Perfection V750 PRO scanner (EPSON Deutschland GmbH, Meerbusch, Germany) at a final pixel resolution of 0.363 nm.

b. Image analysis and processing of 1 mM samples of PDC in binary water/THF mixture

As stated in the paper a closer look at the elongated aggregates which are formed in the binary water/THF mixture (70:30, v/v) uncovered the slight lateral growth with time. To confirm this impression image processing and statistical methods were applied to the cryo-TEM data of the fresh preparation as well as of preparations from 6 and 26 days aged samples. Thereto, isolated sections of the elongated aggregates were extracted from the digitized electron micrographs. These sections were handled like single particles, i.e. they were appropriately band-pass filtered to remove disadvantageous illumination ramps and noise. After careful rotational and translational alignment, they were treated by multivariate statistical analysis (MSA) and finally assigned to different classes according to their most pronounced differences (classification).[2, 3, 4] So-called class sum images, generated by summing up all images of each class, reveal the single particles with improved signal to noise ratio. Thus, variations in size and, if present, shape of the assemblies can now be monitored more easily by comparing the different class sum images. The total sum of all aligned single particle images, on the other hand, displays the mean appearance of the assemblies.

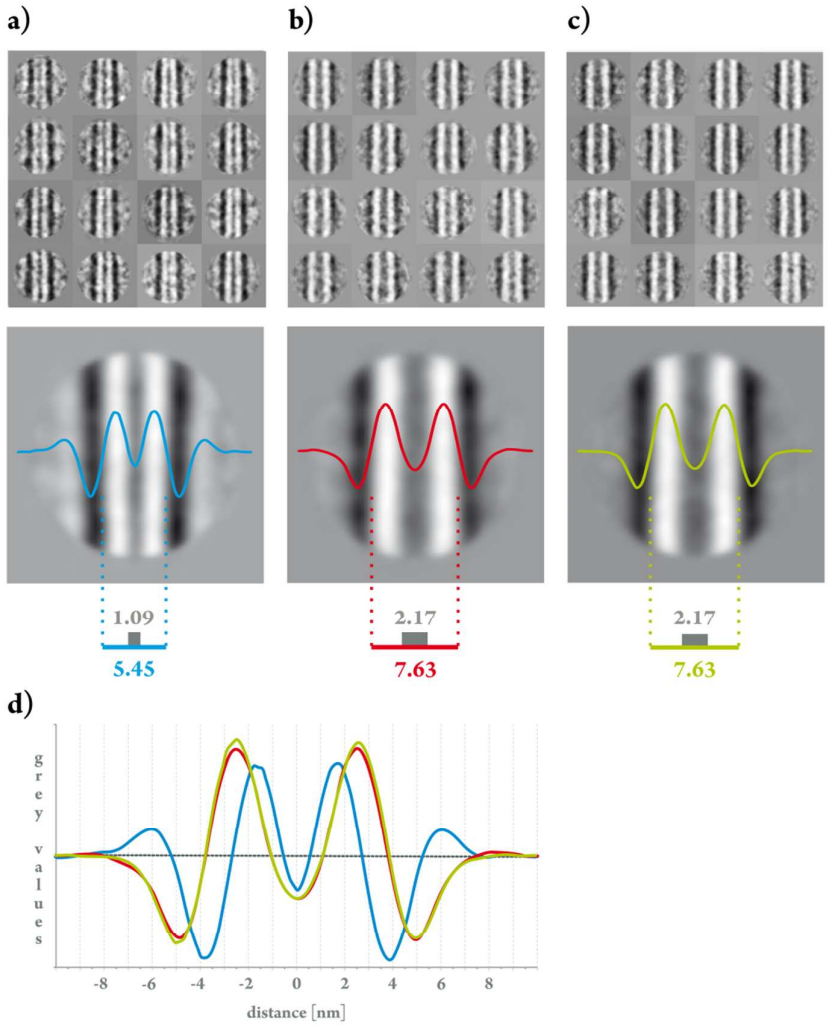

Figure SI 18: Image processing of the electron microscopical data of a 1mM solution of the **PDC** salt directly dissolved in water/THF (70:30, v/v). Note, that the densities are inversed to meet the conventions of image processing. a) – c) The galleries of selected class sum images of the elongated aggregates (upper row), attained from electron micrographs recorded immediately after preparation (a), as well as after 6 (b) and 26 days (c), illustrate the variations of the aggregates diameters within each sample. The total sum images in the lower row additionally indicate the growth of the aggregates diameter with time (distances are given in nanometre). d) The distinct lateral growth can be directly compared by the plots of the grey scale values along the cross sections of the aggregates. Here, the blue line represents the total sum immediately after solvation, while the red and the green line represent the sample after 6 and 26 days, respectively. The coincidence of the latter graphs also proves that the growth of the assemblies is obviously finished within one week.

Densities of images are reversed to meet the conventions of image processing. Three galleries of class sum images from preparations of a 1 mM sample of **PDC** in water/THF (70:30, v/v) immediately after solution, after 6 days and after 26 days, respectively, are shown in Figure SI 18 (a to c, upper row). The class sum images not only indicate a considerable growth of the aggregates diameters with time but also show marked variations of the diameters within each data set. Even a slight proliferation of these variations after one week is to be denoted. Total sum images from all single particles of each preparation are shown below the class sum galleries (Figure SI 18 a to c, lower row). They are overlain with plots of the grey scale values

averaged along the aggregates long axis. These plots are also shown in the diagram in Figure SI 18 d. Here, the dashed dark grey line approximately indicates the mean grey value of the background. Crossings of the graphs with this base line are taken for the measure of the distances from the centre of the total sum image. Starting from the ends of the plots, the first steep decreases on both sides of the aggregates indicate small Fresnel fringes caused by the defocus necessary to achieve proper contrast in the original micrographs. The blue plot, however, starts with a slight increase indicating neighbouring assemblies which could not be averaged out during data accumulation as a result of the close arrangement of the aggregates immediately after preparation of the sample. The next two crossings with the base line delimit the electron dense (high contrast) outer region of the aggregates. In between them, there exists a region of low density (low contrast), which is assumed to be the assemblies core region.

Table SI 1: Graphical analysis of the class sum images derived from MSA and classification provide the ranges of the aggregates size variations and their evolution with time. Values are given in nanometres.

	after 0 days			**after 6 days**			**after 26 days**		
	min	max	average	min	max	average	Min	max	average
outer region	2.00	2.43	2.17	2.46	2.83	2.70	2.56	2.83	2.67
inner region	0.46	1.41	1.02	1.59	2.64	2.24	1.36	2.73	2.12
diameter	4.87	5.81	5.38	6.75	8.31	7.55	6.53	8.22	7.48

Values for the aggregates diameters, the widths of their electron dense outer regions, as well as their inner regions of low contrast are given in Table SI 1. They provide the numerical magnitude of the aforementioned visual inspections, i.e. the individual values clearly show that the mean diameter of the aggregates grows about 2.2 nm (~41%, from 5.4 to 7.6 nm) while the inner region grows from 1.0 to 2.2 nm (~100%) within the first six days. Further growth beyond this time, however, cannot be observed.

c. Crystallisation of PDC from water/THF

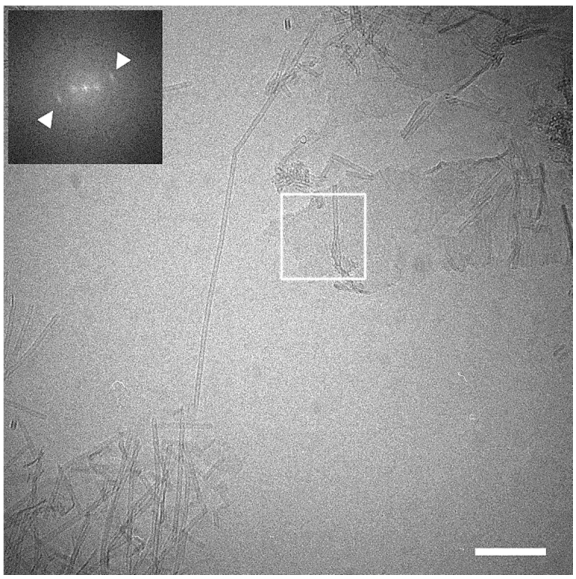

Figure SI 19: Cryo-TEM micrograph of 26 days aged sample of **PDC** in water/THF (70:30, v/v). Next to elongated assemblies (bottom left) sheet-like structures (top right) of different size are observed exhibiting regular layer lines. A Fast Fourier Transform (FFT, upper left corner) of the striated area depicted by the white frame features sharp reflexes that proof a repetitive line distance of 1.95 nm. Scalebar marks 100 nm.

IV. Molecular Modelling

Atomistic Molecular Dynamics (MD) simulations were performed using the Amber 12 suite of programs [5]. The force field parameters for **PDC** are based on the General Amber Force Field (GAFF) [6] and special care was taken to ensure correct behavior of the dihedral rotation for the connection of the calixarene and the perylene subunit of **PDC**. For that reason this dihedral was scanned by single point calculations at the MP2/6-31G* level of theory for a given Fragment of **PDC** (see Figure SI 20) and the force filed barrier was adjusted to give a proper description within an energy range of 20 kcal/mol. Additionally, the improper torsional barrier for the deprotonated carboxylates was adjusted to 10.5 kcal/mol in order to compensate a misbehavior of the force field.

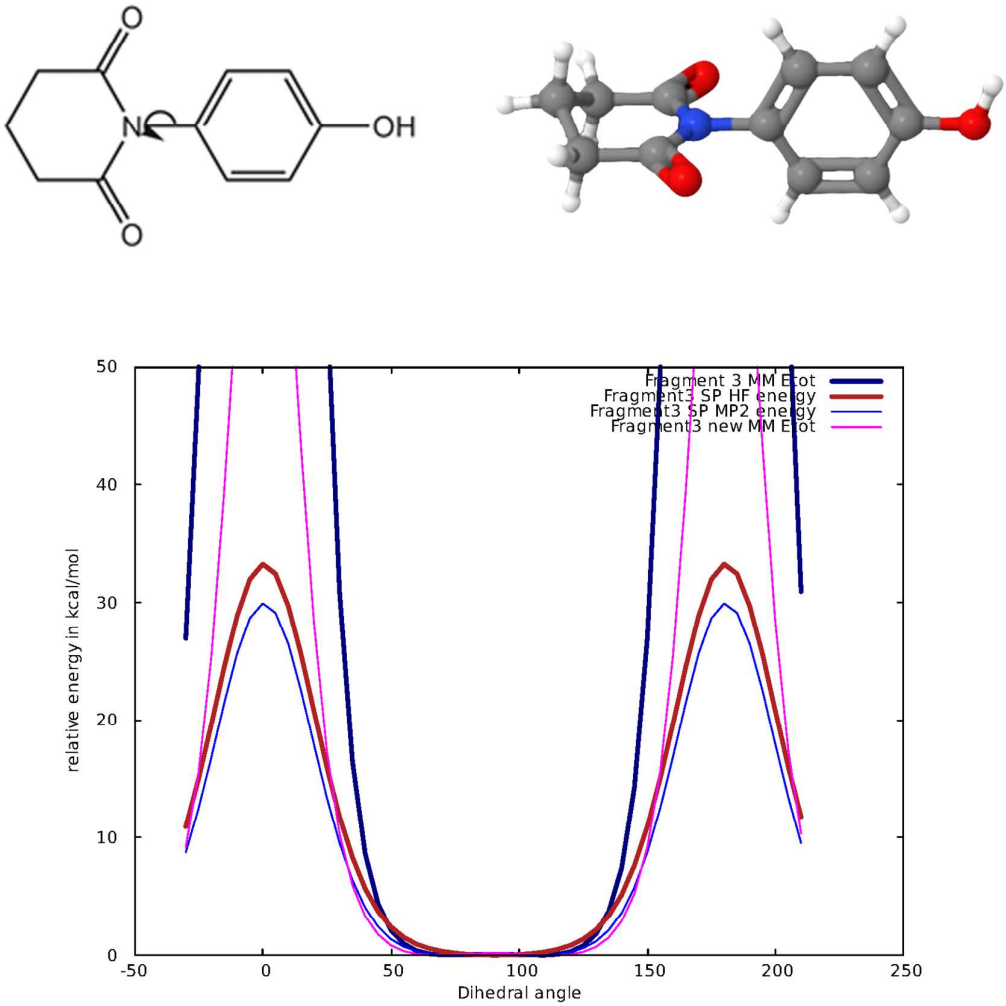

Figure SI 20: Model structure chosen dihedral scan of the perylene calixarene connection and the plot of relative energy against the dihedral angle in degrees (for ab initio calculation, original and fitted force field).

All carboxylates of **PDC** were treated deprotonated leading to a net charge of -6, which was compensated by potassium (or sodium counterions) for simulating in explicit water. The ion parameters were taken from

Joung and Cheatham.[7] The atomic charges of PDC were derived using restrained electrostatic potential (RESP) fitting procedure by Kollman *et al.*[8]. PDC was geometrically optimized *in vacuo* at the BP/def2-SVP level of theory and the charges were derived at the HF/6-31G* level (using Gaussian 09[9]). Due to the size of PDC the molecule was split into 2 fragments and the charges where fitted subsequently. The Fragments chosen for the generation of RESP charges are shown in Figure SI 21. All atom types and modifications to the general Amber force field can be depicted from Table SI 2 and Table SI 3

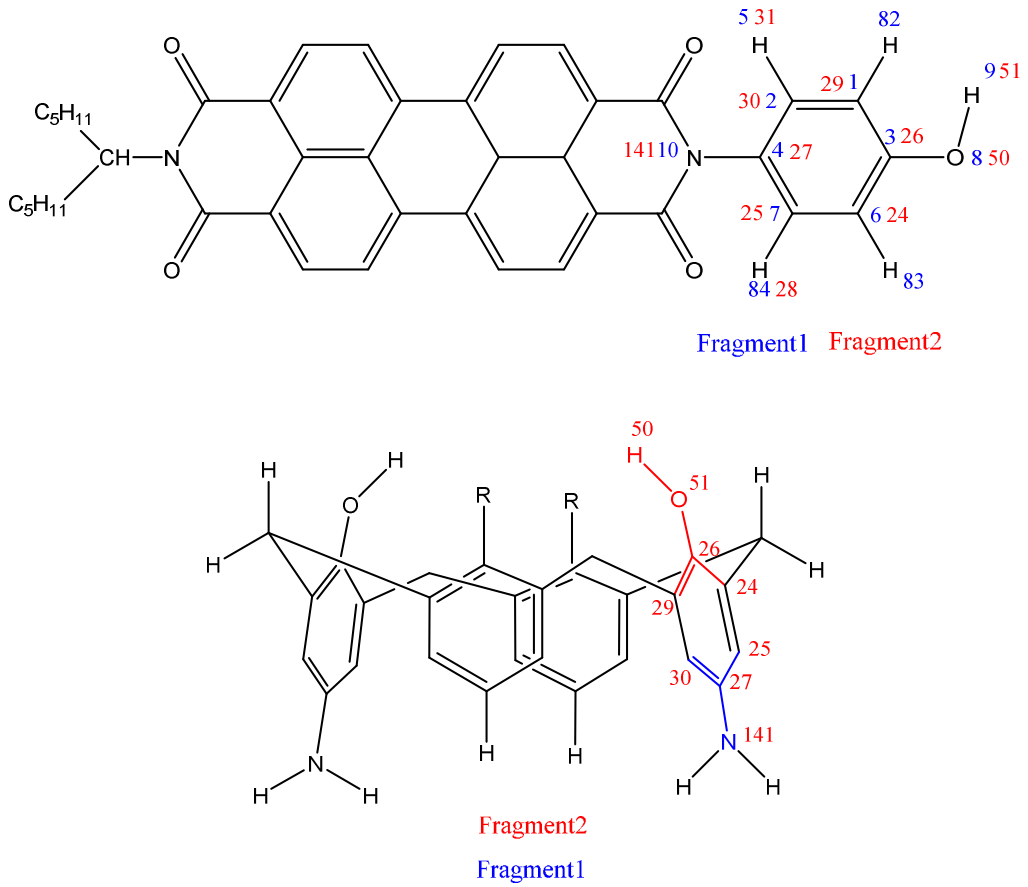

Figure SI 21: The two fragments of **PDC** chosen for RESP charge generation.

Table SI 2: Structure in Cartesian coordinates, GAFF atom types and RESP charges of **PDC** (with carboxylates deprotonated)

1	C1	-2.49	-2.136	-1.413	ca	-0.191662	58	H23	-1.681	-5.638	-3.989	hc	0.058282
2	C2	-3.469	-1.128	-1.368	ca	-0.271661	59	H24	-0.723	-4.481	-4.95	hc	0.058282
3	C3	-3.999	-0.679	-0.151	ca	0.289589	60	H25	0.598	-6.424	-5.932	hc	0.266767
4	C4	-3.531	-1.229	1.054	ca	-0.271661	61	H26	-0.509	-7.56	-5.12	hc	0.266767
5	C5	-2.555	-2.236	1.053	ca	-0.191662	62	C32	0.596	-5.181	3.655	c3	0.171911
6	C6	-2.049	-2.712	-0.19	ca	0.361267	63	H27	0.889	-6.169	3.241	h1	-0.011523
7	H1	-3.824	-0.684	-2.31	hx	0.193176	64	H28	1.418	-4.838	4.326	h1	-0.011523
8	H2	-3.944	-0.875	2.011	hx	0.193176	65	C33	-0.709	-5.275	4.442	c3	0.306865
9	C7	-1.988	-2.8	2.345	c3	-0.016359	66	H29	-1.516	-5.666	3.787	hc	0.058282
10	H3	-1.859	-3.892	2.239	hc	0.039249	67	H30	-1.029	-4.266	4.775	hc	0.058282
11	H4	-2.709	-2.618	3.168	hc	0.039249	68	C34	-0.573	-6.155	5.689	c3	-1.046039
12	C8	-0.642	-2.176	2.707	ca	0.049578	69	H31	-0.405	-7.222	5.422	hc	0.266767
13	C9	-0.544	-0.79	2.945	ca	-0.242606	70	H32	0.319	-5.84	6.278	hc	0.266767
14	C10	0.552	-2.932	2.758	ca	0.18149	71	C35	-1.788	-6.007	6.624	c	0.824248
15	C11	0.691	-0.179	3.203	ca	-0.156849	72	O5	-2.409	-4.945	6.71	o	-0.579564
16	H5	-1.458	-0.178	2.905	ha	0.150944	73	N1	-2.075	-7.12	7.37	n	-1.081853
17	C12	1.821	-2.329	2.948	ca	0.049578	74	H33	-1.534	-7.965	7.177	hn	0.377478
18	C13	1.867	-0.942	3.184	ca	-0.242606	75	C36	-1.388	-6.342	-6.729	c	0.824248
19	H6	0.74	0.905	3.391	ha	0.130348	76	O6	-1.702	-5.217	-7.127	o	-0.579564
20	H7	2.844	-0.455	3.332	ha	0.150944	77	N2	-1.836	-7.504	-7.3	n	-1.081853
21	C14	3.116	-3.124	2.795	c3	-0.016359	78	H34	-1.483	-8.381	-6.913	hn	0.377478
22	H8	3.837	-2.792	3.568	hc	0.039249	79	C37	-3.173	-7.253	8.365	c3	0.540637
23	H9	2.937	-4.202	2.982	hc	0.039249	80	C38	-2.97	-8.685	8.965	c3	0.958403
24	C15	3.768	-2.951	1.428	ca	-0.191662	81	C39	-3.08	-6.107	9.416	c3	0.958403
25	C16	4.964	-2.222	1.306	ca	-0.271661	82	C40	-4.508	-7.125	7.563	c3	0.958403
26	C17	3.177	-3.498	0.255	ca	0.361267	83	H35	-1.884	-8.833	9.158	hc	-0.344636
27	C18	5.59	-2.048	0.063	ca	0.289589	84	C41	-3.689	-9.071	10.279	c3	-0.268515
28	H10	5.425	-1.796	2.21	hx	0.193176	85	H36	-3.263	-9.412	8.18	hc	-0.344636
29	C19	3.787	-3.289	-1.015	ca	-0.191662	86	H37	-3.403	-5.171	8.918	hc	-0.344636
30	C20	4.999	-2.59	-1.09	ca	-0.271661	87	H38	-3.803	-6.313	10.227	hc	-0.344636
31	H11	5.481	-2.447	-2.068	hx	0.193176	88	C42	-1.678	-5.864	10.019	c3	-0.268515
32	C21	3.065	-3.759	-2.266	c3	-0.016359	89	H39	-4.478	-6.128	7.082	hc	-0.344636
33	H12	3.801	-3.859	-3.092	hc	0.039249	90	H40	-4.485	-7.879	6.749	hc	-0.344636
34	H13	2.626	-4.755	-2.076	hc	0.039249	91	C43	-5.84	-7.28	8.309	c3	-0.268515
35	C22	1.964	-2.78	-2.677	ca	0.049578	92	H41	-4.769	-8.841	10.282	hc	-0.047497
36	C23	2.286	-1.438	-2.963	ca	-0.242606	93	H42	-3.584	-10.169	10.398	hc	-0.047497
37	C24	0.596	-3.144	-2.697	ca	0.18149	94	C44	-3.018	-8.41	11.475	c	0.820659
38	C25	1.285	-0.491	-3.231	ca	-0.156849	95	H43	-1.19	-6.825	10.288	hc	-0.047497
39	H14	3.338	-1.116	-2.924	ha	0.150944	96	H44	-1.026	-5.335	9.299	hc	-0.047497
40	C26	-0.434	-2.195	-2.906	ca	0.049578	97	C45	-1.72	-5.072	11.311	c	0.820659
41	C27	-0.065	-0.863	-3.179	ca	-0.242606	98	H45	-5.839	-6.836	9.326	hc	-0.047497
42	H15	1.562	0.552	-3.445	ha	0.130348	99	H46	-6.633	-6.72	7.764	hc	-0.047497
43	H16	-0.853	-0.109	-3.333	ha	0.150944	100	C46	-6.349	-8.709	8.389	c	0.820659
44	C28	-1.903	-2.573	-2.748	c3	-0.016359	101	O7	-1.826	-8.521	11.719	o	-0.8318
45	H17	-2.49	-2.1	-3.561	hc	0.039249	102	O8	-3.855	-7.619	12.178	o	-0.8318
46	H18	-2.022	-3.668	-2.871	hc	0.039249	103	O9	-2.366	-5.354	12.317	o	-0.8318
47	O1	0.21	-4.447	-2.372	os	-0.29096	104	O10	-0.927	-3.979	11.279	o	-0.8318
48	O2	-1.154	-3.725	-0.111	oh	-0.576899	105	O11	-5.962	-9.648	7.717	o	-0.8318
49	O3	0.512	-4.309	2.505	os	-0.29096	106	O12	-7.35	-8.829	9.303	o	-0.8318
50	O4	2.044	-4.235	0.25	oh	-0.576899	107	C47	-2.681	-7.614	-8.52	c3	0.540637
51	H19	1.584	-4.31	1.128	ho	0.383461	108	C48	-2.919	-9.152	-8.68	c3	0.958403
52	H20	-0.803	-4.038	-0.983	ho	0.383461	109	C49	-3.987	-6.785	-8.333	c3	0.958403
53	C29	0.392	-5.474	-3.368	c3	0.171911	110	C50	-1.84	-7.014	-9.692	c3	0.958403
54	C30	-0.685	-5.472	-4.452	c3	0.306865	111	H47	-3.146	-9.579	-7.678	hc	-0.344636
55	H21	0.394	-6.428	-2.801	h1	-0.011523	112	C51	-4.041	-9.657	-9.617	c3	-0.268515
56	H22	1.398	-5.358	-3.831	h1	-0.011523	113	H48	-1.959	-9.599	-9.013	hc	-0.344636
57	C31	-0.437	-6.531	-5.534	c3	-1.046039	114	H49	-3.714	-5.714	-8.398	hc	-0.344636

115	H50	-4.666	-7.003	-9.18	hc	-0.344636
116	C52	-4.734	-7.005	-6.998	c3	-0.268515
117	H51	-1.625	-5.965	-9.407	hc	-0.344636
118	H52	-0.868	-7.55	-9.717	hc	-0.344636
119	C53	-2.425	-7.036	-11.111	c3	-0.268515
120	H53	-4.024	-9.2	-10.622	hc	-0.047497
121	H54	-3.89	-10.749	-9.749	hc	-0.047497
122	C54	-5.408	-9.453	-8.98	c	0.820659
123	H55	-4.796	-8.086	-6.751	hc	-0.047497
124	H56	-4.216	-6.49	-6.169	hc	-0.047497
125	C55	-6.174	-6.531	-7.043	c	0.820659
126	H57	-3.517	-6.848	-11.149	hc	-0.047497
127	H58	-1.981	-6.204	-11.704	hc	-0.047497
128	C56	-2.107	-8.296	-11.898	c	0.820659
129	O13	-5.701	-9.884	-7.875	o	-0.8318
130	O14	-6.223	-8.673	-9.719	o	-0.8318
131	O15	-7.033	-6.891	-7.844	o	-0.8318
132	O16	-6.464	-5.65	-6.063	o	-0.8318
133	O17	-1.251	-9.118	-11.622	o	-0.8318
134	O18	-2.885	-8.398	-13.008	o	-0.8318
135	N3	6.817	-1.287	-0.033	n	-0.282779
136	C57	6.805	-0.117	-0.841	c	0.619564
137	C58	7.948	-1.755	0.689	c	0.619564
138	C59	8.062	0.683	-0.874	ca	-0.178372
139	O19	5.806	0.218	-1.47	o	-0.53425
140	C60	9.18	-0.919	0.614	ca	-0.178372
141	O20	7.902	-2.79	1.345	o	-0.53425
142	C61	9.22	0.28	-0.152	ca	0.067141
143	C62	8.095	1.859	-1.629	ca	-0.052214
144	C63	10.317	-1.324	1.318	ca	-0.052214
145	C64	10.417	1.078	-0.194	ca	0.060887
146	C65	9.258	2.644	-1.675	ca	-0.22256
147	H59	7.187	2.149	-2.179	ha	0.162606
148	C66	11.491	-0.552	1.282	ca	-0.22256
149	H60	10.264	-2.256	1.9	ha	0.162606
150	C67	10.427	2.287	-0.974	ca	0.03858
151	C68	11.573	0.647	0.546	ca	0.03858
152	H61	9.24	3.562	-2.278	ha	0.167351
153	H62	12.361	-0.906	1.852	ha	0.167351
154	C69	11.649	3.106	-1.011	ca	0.042849
155	C70	12.793	1.469	0.514	ca	0.042849
156	C71	12.802	2.68	-0.263	ca	0.067511
157	C72	11.734	4.302	-1.752	ca	-0.227607
158	C73	13.96	1.117	1.221	ca	-0.227607
159	C74	13.993	3.487	-0.291	ca	0.006349
160	C75	12.902	5.082	-1.776	ca	-0.068682
161	H63	10.868	4.649	-2.333	ha	0.169317
162	C76	15.118	1.912	1.189	ca	-0.068682
163	H64	13.98	0.198	1.822	ha	0.169317
164	C77	14.031	4.688	-1.053	ca	-0.104198
165	C78	15.147	3.093	0.442	ca	-0.104198
166	H65	12.955	6.013	-2.359	ha	0.167492
167	H66	16.022	1.628	1.747	ha	0.167492
168	C79	15.253	5.539	-1.095	c	0.547043
169	C80	16.388	3.918	0.431	c	0.547043
170	N4	16.364	5.103	-0.331	n	-0.307459
171	O21	15.296	6.574	-1.758	o	-0.545375
172	O22	17.391	3.587	1.063	o	-0.545375
173	C81	17.591	5.955	-0.369	c3	0.393182
174	C82	18.71	5.236	-1.156	c3	-0.388159
175	H67	17.262	6.827	-0.969	h1	0.038105
176	C83	19.939	6.104	-1.461	c3	0.074597
177	H68	19.022	4.331	-0.595	hc	0.115694
178	H69	18.275	4.884	-2.118	hc	0.115694
179	C84	20.981	5.385	-2.33	c3	-0.011458
180	H70	19.62	7.043	-1.97	hc	-0.002372
181	H71	20.423	6.422	-0.511	hc	-0.002372
182	H72	21.288	4.439	-1.828	hc	0.005659
183	H73	20.508	5.072	-3.29	hc	0.005659
184	C85	22.229	6.228	-2.632	c3	0.121818
185	C86	23.264	5.505	-3.502	c3	-0.225532
186	H74	22.701	6.538	-1.671	hc	-0.019694
187	H75	21.919	7.175	-3.129	hc	-0.019694
188	H76	23.623	4.574	-3.015	hc	0.050709
189	H77	22.835	5.217	-4.485	hc	0.050709
190	N5	-5.015	0.351	-0.138	n	-0.282779
191	C87	-6.309	-0.006	0.325	c	0.619564
192	C88	-4.649	1.644	-0.597	c	0.619564
193	C89	-7.338	1.074	0.325	ca	-0.178372
194	O23	-6.56	-1.146	0.702	o	-0.53425
195	C90	-5.718	2.684	-0.578	ca	-0.178372
196	O24	-3.512	1.884	-0.989	o	-0.53425
197	C91	-7.034	2.39	-0.124	ca	0.067141
198	C92	-8.629	0.779	0.771	ca	-0.052214
199	C93	-5.413	3.975	-1.018	ca	-0.052214
200	C94	-8.048	3.412	-0.12	ca	0.060887
201	C95	-9.624	1.77	0.78	ca	-0.22256
202	H78	-8.839	-0.246	1.112	ha	0.162606
203	C96	-6.396	4.979	-1.018	ca	-0.22256
204	H79	-4.388	4.179	-1.363	ha	0.162606
205	C97	-9.37	3.087	0.345	ca	0.03858
206	C98	-7.713	4.733	-0.581	ca	0.03858
207	H80	-10.626	1.496	1.139	ha	0.167351
208	H81	-6.114	5.98	-1.372	ha	0.167351
209	C99	-10.406	4.132	0.35	ca	0.042849
210	C100	-8.751	5.776	-0.584	ca	0.042849
211	C101	-10.073	5.451	-0.117	ca	0.067511
212	C102	-11.721	3.889	0.796	ca	-0.227607
213	C103	-8.501	7.089	-1.03	ca	-0.227607
214	C104	-11.088	6.471	-0.118	ca	0.006349
215	C105	-12.705	4.892	0.792	ca	-0.068682
216	H82	-12.001	2.891	1.16	ha	0.169317
217	C106	-9.499	8.078	-1.031	ca	-0.068682
218	H83	-7.501	7.363	-1.393	ha	0.169317
219	C107	-12.403	6.179	0.34	ca	-0.104198
220	C108	-10.788	7.783	-0.58	ca	-0.104198
221	H84	-13.727	4.689	1.142	ha	0.167492
222	H85	-9.292	9.099	-1.384	ha	0.167492
223	C109	-13.468	7.22	0.345	c	0.547043
224	C110	-11.827	8.852	-0.595	c	0.547043
225	N6	-13.108	8.51	-0.117	n	-0.307459
226	O25	-14.61	6.973	0.733	o	-0.545375
227	O26	-11.581	9.988	-1.002	o	-0.545375
228	C111	-14.177	9.553	-0.125	c3	0.393182
229	C112	-14.592	9.869	-1.58	c3	-0.388159
230	H86	-15.025	9.034	0.364	h1	0.038105
231	C113	-15.839	10.755	-1.715	c3	0.074597
232	H87	-13.737	10.346	-2.103	hc	0.115694
233	H88	-14.785	8.902	-2.094	hc	0.115694
234	C114	-16.276	10.955	-3.174	c3	-0.011458

235	H89	-16.681	10.31	-1.137	hc	-0.002372
236	H90	-15.647	11.751	-1.258	hc	-0.002372
237	H91	-15.428	11.385	-3.755	hc	0.005659
238	H92	-16.48	9.962	-3.636	hc	0.005659
239	C115	-17.511	11.854	-3.337	c3	0.121818
240	C116	-17.943	12.045	-4.795	c3	-0.225532
241	H93	-17.303	12.846	-2.876	hc	-0.019694
242	H94	-18.354	11.424	-2.751	hc	-0.019694
243	H95	-17.135	12.509	-5.4	hc	0.050709
244	H96	-18.196	11.075	-5.273	hc	0.050709
245	C117	17.988	6.462	1.043	c3	-0.388159
246	C118	18.367	7.953	1.081	c3	0.074597
247	H97	18.812	5.839	1.45	hc	0.115694
248	H98	17.133	6.304	1.735	hc	0.115694
249	C119	18.775	8.438	2.479	c3	-0.011458
250	H99	19.197	8.155	0.369	hc	-0.002372
251	H100	17.507	8.558	0.716	hc	-0.002372
252	C120	19.141	9.929	2.539	c3	0.121818
253	H101	17.947	8.234	3.197	hc	0.005659
254	H102	19.637	7.833	2.842	hc	0.005659
255	H103	19.968	10.131	1.821	hc	-0.019694
256	H104	18.279	10.531	2.176	hc	-0.019694
257	C121	19.549	10.407	3.938	c3	-0.225532
258	H105	19.806	11.486	3.944	hc	0.050709
259	H106	18.729	10.255	4.672	hc	0.050709
260	H107	20.433	9.85	4.314	hc	0.050709
261	H108	24.151	6.142	-3.699	hc	0.050709
262	C122	-13.796	10.781	0.744	c3	-0.388159
263	C123	-14.941	11.287	1.638	c3	0.074597
264	H109	-13.418	11.599	0.096	hc	0.115694
265	H110	-12.941	10.507	1.398	hc	0.115694
266	C124	-14.558	12.515	2.476	c3	-0.011458
267	H111	-15.832	11.532	1.019	hc	-0.002372
268	H112	-15.267	10.465	2.316	hc	-0.002372
269	C125	-15.684	13.025	3.387	c3	0.121818
270	H113	-13.663	12.274	3.095	hc	0.005659
271	H114	-14.234	13.337	1.796	hc	0.005659
272	H115	-16.576	13.263	2.766	hc	-0.019694
273	H116	-16.005	12.203	4.066	hc	-0.019694
274	C126	-15.294	14.254	4.218	c3	-0.225532
275	H117	-16.129	14.595	4.863	hc	0.050709
276	H118	-14.428	14.037	4.879	hc	0.050709
277	H119	-15.005	15.107	3.568	hc	0.050709
278	H120	-18.836	12.699	-4.876	hc	0.050709

Table SI 3: Modifications to the standard GAFF parameters for **PDC**

MASS					
Hx		1.008	0.135		included hx for vdW trimming
BOND					
ca-hx			344.30	1.087	set to ca-ha s.a.
ANGLE					
ca-ca-hx		48.460	120.010		same as ca-ca-ha s.a.
DIHE					
ca-ca-ca-hx	1	3.625	180.000	2.000	
hx-ca-ca-c3	1	3.625	180.000	2.000	
hx-ca-ca-n	1	3.625	180.000	2.000	
IMPROPER					
ca-ca-ca-hx		1.1	180.0	2.0	Using default value
ca-ca-ca-n		1.1	180.0	2.0	Using default value
ca-ca-ca-oh		1.1	180.0	2.0	Using default value
ca-ca-ca-ha		1.1	180.0	2.0	General improper torsional angle (2 general atom types)
ca-ca-ca-os		1.1	180.0	2.0	Using default value
c3-n -c –o		10.5	180.0	2.0	General improper torsional angle (2 general atom types)
c -c3-n –hn		1.1	180.0	2.0	
c3-o -c –o		10.5	180.0	2.0	!! corrected Improper for deprotonated COO- (cmj) !!
c -c -n –ca		1.1	180.0	2.0	Using default value
ca-n -c –o		10.5	180.0	2.0	General improper torsional angle (2 general atom types)
c -ca-ca-ca		1.1	180.0	2.0	Using default value
ca-ca-ca-ca		1.1	180.0	2.0	Using default value
c -c -n -c3		1.1	180.0	2.0	Using default value
NONBON					
Hx		1.1000	0.0157		

a. MD simulation

Each system was minimized in two steps: a combined steepest descend and conjugate gradient minimization for a maximum of 1000 cycles with all solute atoms restrained in their positions followed by a free minimization for a maximum of 5000 cycles. Subsequently all systems containing explicit water were heated from 0 to 300 K for 50 ps using a Langevin dynamics thermostat (again with positional restraints on the solute atoms), followed by 5 ns equilibration of free Langevin directed dynamics and at least 100 ns constant pressure dynamics (NPT) at 1 Atmosphere. Electrostatic interactions were treated using the particle mesh Ewald (PME) method[10] and a 10 Å distance cutoff for non-bonded interactions. The SPC/E water model[11] was chosen for explicit water treatment together with periodic boundary conditions in a truncated octahedral box. The integration time step during all simulations was set to 1 fs.

The monomers were simulated as open and closed conformation and showed to be stable in their conformation for a simulation time of at least 100 ns. To simulate the interactions of the x-shaped monomer with other monomers simulations of 6 monomers were performed. The PDC molecules were placed randomly in the box and the box was filled with SPC/E water with a minimal distance of the solutes to the boundary of the box of 15 Å.

In these simulations formation of dimers and trimers could be detected. The individual dimers once formed, were stable throughout the rest of the simulation time (between 50 and 150ns).

b. Umbrella Sampling

In order to retrieve the relative free energy differences between the t-shaped and the x-shaped monomer of PDC Umbrella Sampling (US) simulations were applied followed by the weighted histogram analysis method (WHAM)[12] to retrieve the potential of mean force, or the change in free energy, along the given reaction coordinate. The distance between the alkyl-substituted terminal nitrogen atoms of the perylene moieties was chosen as reaction coordinate providing full rotational flexibility of the perylene moieties to each other upon conformational change.

To follow this given reaction coordinate a so called harmonic Umbrella potential was applied in form of a specific restraint to the simulation. For the monomer in water the reaction coordinate (N-N distance) was scanned between 4.0 and 32.0 Å in 0.1 Å steps. To ensure proper simulation each window was sampled for 6 ns starting from similar starting coordinates. Distance measurements were performed every 500 fs. The spring constant of the Umbrella potential was adjusted to 5.0 kcal/mol$Å^2$ in the flat free energy regime and to 10.0 kcal/mol$Å^2$ in the area of the transition between the two conformers, again to ensure proper structural sampling.

V. Crystallogarphic Data of Dibutanoic acid methylester-calix[4]arene 5

a. General Procedure

A solution of the Dibutanoic acid methylester-calix[4]arene 5 in CH_2Cl_2 was concentrated over a period of 2 weeks to afford single crystals of compound 5.

b. Crystallographic Data

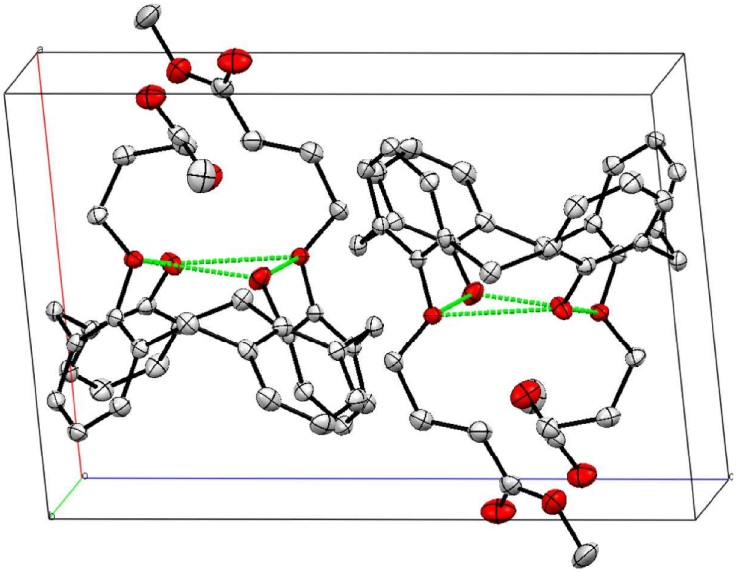

Figure SI 22: Elementary cell of Dibutanoic acid methylester-calix[4]arene **5**.

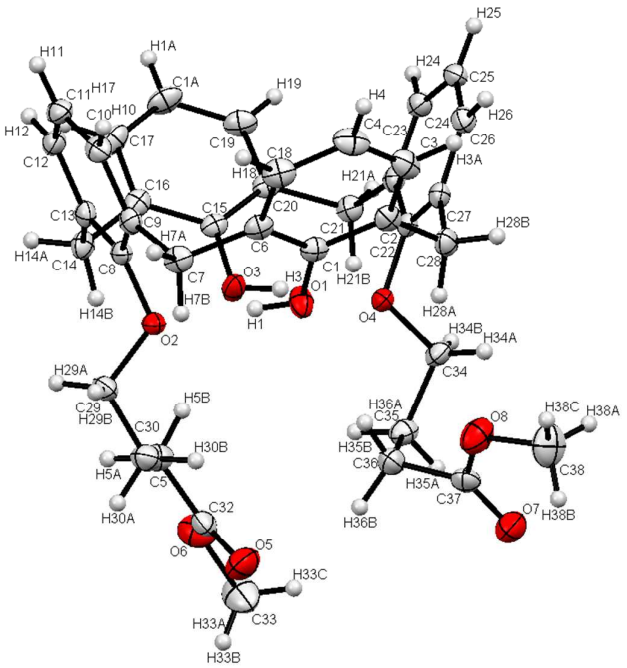

Identification code	FR01	m/mm^{-1}	0.093
Empirical formula	$C_{38}H_{40}O_8$	F(000)	664.0
Formula weight	624.70	Crystal size/mm^3	0.3557 × 0.2655 × 0.2267
Temperature/K	173.00(14)	2Θ range for data collection	5.64 to 59.26°
radiation wavelength	1.5418 (Cu Kα)	Index ranges	-13 ≤ h ≤ 12 -14 ≤ k ≤ 15 -19 ≤ l ≤ 20
Crystal system	triclinic		
Space group	P-1		
a/Å	9.7356(5)	Reflections collected	15087
b/Å	11.2251(4)	Independent reflections	7362[R(int) = 0.0221]
c/Å	14.6888(6)	Data/restraints/parameters	7362/0/419
α/°	97.369(3)	Goodness-of-fit on F^2	1.042
β/°	95.733(4)	Final R indexes [I ≥ 2σ (I)]	R_1 = 0.0515, wR_2 = 0.1214
γ/°	99.239(4)	Final R indexes [all data]	R_1 = 0.0647, wR_2 = 0.1319
Volume/Å^3	1559.39(12)	Largest diff. peak/hole / e Å^{-3}	0.79/-0.32
Z	2		
ρ_{calc}mg/mm^3	1.330		

Table SI 4: Fractional Atomic Coordinates (×104) and Equivalent Isotropic Displacement Parameters (Å2×103). Ueq is defined as 1/3 of of the trace of the orthogonalised UIJ tensor.

	x	*y*	*z*	U(eq)		*x*	*y*	*z*	U(eq)
O1	5064.7(13)	3868.4(11)	3301.7(8)	26.8(3)	C15	4085.8(16)	407.2(14)	1306.2(11)	18.6(3)
O2	5368.9(11)	1680.1(10)	3830.5(7)	19.6(2)	C16	3567.9(18)	-585.7(14)	1742.5(11)	21.0(3)
O3	5154.1(13)	1242.6(10)	1806.3(8)	25.1(3)	C17	2492.0(19)	-1472.2(15)	1257.3(12)	27.0(4)
O4	5469.7(11)	3535.5(10)	1359.4(7)	19.8(2)	C18	2302.6(19)	4704.3(16)	4649.2(12)	27.8(4)
O5	10061.5(16)	2747.6(13)	3194.9(12)	44.2(4)	C19	2460.9(19)	-401.2(16)	-50.0(12)	26.3(4)
O6	9675.5(15)	999.8(14)	2216.4(10)	39.9(3)	C20	3538.2(17)	512.6(14)	406.8(11)	19.8(3)
O7	9587.1(15)	6570.1(12)	2064.9(10)	38.0(3)	C21	4072.0(18)	1601.9(14)	-55.9(11)	21.3(3)
O8	7695.7(15)	6630.1(12)	2806.1(10)	38.3(3)	C22	4119.0(17)	3619.4(14)	984.3(11)	19.1(3)
C1	3981.7(17)	4378.7(14)	3600.0(11)	20.5(3)	C23	3430.7(17)	2708.2(14)	267.9(10)	20.0(3)
C1A	1937(2)	-1386.8(16)	368.6(13)	30.2(4)	C24	2090.3(18)	2806.4(15)	-111.1(11)	22.4(3)
C2	3507.9(18)	5220.6(14)	3072.1(11)	21.9(3)	C25	1450.2(17)	3765.0(15)	225.0(11)	23.4(3)
C3	2420.2(19)	5789.8(15)	3351.7(12)	27.2(4)	C26	2119.9(18)	4613.8(15)	967.1(11)	23.4(3)
C4	1817(2)	5534.9(16)	4135.3(13)	30.2(4)	C27	3471.7(17)	4558.2(14)	1366.4(11)	20.3(3)
C5	8043.0(19)	1238.6(17)	3262.9(13)	29.7(4)	C28	4157.8(19)	5474.6(14)	2203.6(11)	23.3(3)
C6	3384.0(18)	4109.7(14)	4396.8(11)	21.6(3)	C29	6442.6(17)	1422.0(16)	4492.9(11)	24.1(3)
C7	3876.3(18)	3172.3(15)	4953.9(11)	22.7(3)	C30	7832.9(19)	1900.0(17)	4186.3(12)	29.1(4)
C8	4000.8(16)	1180.1(14)	3937.7(10)	18.6(3)	C32	9355.9(19)	1759.8(16)	2906.2(12)	26.5(4)
C9	3261.9(17)	1873.7(14)	4505.1(10)	20.3(3)	C33	10967(2)	1459(2)	1848.1(17)	49.2(6)
C10	1889.6(18)	1366.4(16)	4600.5(11)	23.2(3)	C34	6581.6(17)	4135.1(15)	906.5(11)	22.9(3)
C11	1278.3(18)	219.8(16)	4137.7(11)	24.6(3)	C35	7961.7(18)	3995.3(15)	1415.9(12)	25.5(4)
C12	2015.2(18)	-427.3(15)	3547.8(11)	23.0(3)	C36	8283.1(19)	4696.2(15)	2399.7(12)	27.2(4)
C13	3387.3(17)	44.5(14)	3428.3(10)	19.8(3)	C37	8625.1(18)	6049.9(16)	2397.1(12)	25.6(4)
C14	4140.7(18)	-647.0(14)	2733.9(11)	21.8(3)	C38	7864(3)	7924.8(18)	2794.9(16)	44.0(5)

Table SI 5: Anisotropic Displacement Parameters (Å2×103). The Anisotropic displacement factor exponent takes the form: -2π2[h2a*2U11+...+2hka×b×U12]

	U11	U22	U33	U23	U13	U12		U11	U22	U33	U23	U13	U12
O1	30.7(7)	27.4(6)	28.9(6)	11.6(5)	12.9(5)	13.6(5)	C15	17.2(8)	17.7(7)	20.4(7)	-1.1(6)	4.6(6)	3.0(6)
O2	15.5(5)	24.3(6)	20.0(5)	7.1(4)	2.3(4)	3.4(4)	C16	22.3(8)	18.3(7)	23.0(8)	0.4(6)	7.7(6)	4.9(6)
O3	27.4(7)	20.3(6)	24.0(6)	6.4(5)	-4.1(5)	-4.5(5)	C17	30.1(10)	18.0(8)	31.3(9)	-0.1(7)	9.8(7)	-1.3(7)
O4	16.4(6)	21.9(5)	21.2(5)	7.6(4)	1.6(4)	0.7(4)	C18	27.3(9)	28.9(9)	24.9(8)	-4.7(7)	5.2(7)	4.0(7)
O5	32.5(8)	33.5(7)	65.2(10)	11.7(7)	6.2(7)	-1.9(6)	C19	25.0(9)	29.5(9)	20.2(8)	-5.0(7)	0.2(7)	1.3(7)
O6	37.2(8)	50.5(9)	33.4(7)	1.8(6)	8.2(6)	13.4(7)	C20	19.0(8)	21.2(7)	19.0(7)	-1.1(6)	5.4(6)	4.3(6)
O7	31.8(8)	34.0(7)	49.2(8)	12.6(6)	8.6(6)	1.5(6)	C21	22.2(8)	25.3(8)	15.4(7)	1.1(6)	3.0(6)	2.5(6)
O8	39.9(8)	24.6(6)	50.5(9)	1.1(6)	14.2(7)	4.0(6)	C22	17.6(8)	21.7(7)	19.0(7)	8.5(6)	2.3(6)	1.5(6)
C1	19.7(8)	18.0(7)	21.7(8)	-2.9(6)	1.4(6)	2.5(6)	C23	21.1(8)	22.9(8)	16.8(7)	6.5(6)	4.6(6)	2.2(6)
C1A	26.7(9)	26.4(9)	30.8(9)	-7.2(7)	2.6(7)	-5.7(7)	C24	21.7(8)	26.2(8)	17.8(7)	4.5(6)	0.5(6)	-0.3(6)
C2	24.5(9)	16.3(7)	22.0(8)	-2.6(6)	-1.6(6)	1.9(6)	C25	17.1(8)	29.8(8)	24.7(8)	11.2(7)	0.7(6)	3.3(6)
C3	29.2(9)	20.2(8)	30.6(9)	-2.5(7)	-2.7(7)	7.8(7)	C26	23.3(8)	22.5(8)	26.6(8)	7.4(6)	4.7(7)	6.8(6)
C4	25.7(9)	29.5(9)	34.1(10)	-6.8(7)	2.9(8)	10.7(7)	C27	21.5(8)	19.1(7)	20.9(7)	7.4(6)	3.1(6)	1.4(6)
C5	22.6(9)	32.2(9)	33.3(9)	1.7(7)	2.6(7)	5.2(7)	C28	26.5(9)	16.3(7)	26.5(8)	4.3(6)	0.2(7)	2.7(6)
C6	21.9(8)	20.2(7)	19.4(7)	-3.8(6)	0.8(6)	0.5(6)	C29	20.4(8)	31.3(9)	21.7(8)	8.4(7)	0.3(6)	6.3(7)
C7	23.8(9)	26.4(8)	16.2(7)	-0.9(6)	3.2(6)	2.7(6)	C30	23.0(9)	34.5(9)	28.7(9)	4.8(7)	-0.6(7)	4.2(7)
C8	16.9(8)	23.1(7)	16.9(7)	7.5(6)	2.2(6)	3.2(6)	C32	24.6(9)	29.0(9)	29.7(9)	11.1(7)	2.5(7)	11.1(7)
C9	22.9(8)	23.1(8)	15.3(7)	5.0(6)	1.9(6)	3.7(6)	C33	38.5(12)	76.1(16)	46.8(12)	27.5(12)	24.4(10)	24.8(12)
C10	22.3(9)	29.8(8)	19.4(7)	5.5(6)	5.9(6)	7.0(7)	C34	20.4(8)	24.5(8)	22.5(8)	5.1(6)	4.9(6)	-2.2(6)
C11	19.2(8)	31.4(9)	23.6(8)	8.8(7)	4.1(6)	0.9(7)	C35	20.8(9)	23.4(8)	31.8(9)	1.7(7)	5.4(7)	3.0(6)
C12	23.1(8)	22.2(8)	23.0(8)	6.7(6)	2.7(6)	-0.6(6)	C36	25.1(9)	25.2(8)	30.4(9)	6.5(7)	-1.6(7)	3.2(7)
C13	22.9(8)	20.5(7)	17.4(7)	7.4(6)	2.9(6)	4.1(6)	C37	21.7(9)	27.5(8)	24.7(8)	2.9(7)	-5.3(7)	1.3(7)
C14	25.4(9)	16.6(7)	24.5(8)	3.9(6)	5.9(7)	5.0(6)	C38	60.5(15)	26.1(10)	44.9(12)	-0.8(9)	8.8(11)	9.0(9)

Table SI 6: Bond Lengths

		Length/Å			Length/Å			Length/Å			Length/Å
O1	C1	1.361(2)	C1	C6	1.404(2)	C8	C13	1.401(2)	C22	C23	1.402(2)
O2	C8	1.3922(19)	C1A	C17	1.383(3)	C9	C10	1.394(2)	C22	C27	1.398(2)
O2	C29	1.4456(19)	C1A	C19	1.385(3)	C10	C11	1.386(2)	C23	C24	1.394(2)
O3	C15	1.3632(19)	C2	C3	1.391(2)	C11	C12	1.387(2)	C24	C25	1.389(2)
O4	C22	1.3964(19)	C2	C28	1.519(2)	C12	C13	1.393(2)	C25	C26	1.383(2)
O4	C34	1.4464(19)	C3	C4	1.385(3)	C13	C14	1.520(2)	C26	C27	1.400(2)
O5	C32	1.207(2)	C4	C18	1.383(3)	C14	C16	1.521(2)	C27	C28	1.519(2)
O6	C32	1.333(2)	C5	C30	1.510(3)	C15	C16	1.405(2)	C29	C30	1.508(2)
O6	C33	1.463(3)	C5	C32	1.491(3)	C15	C20	1.401(2)	C34	C35	1.512(2)
O7	C37	1.202(2)	C6	C7	1.520(2)	C16	C17	1.389(2)	C35	C36	1.531(2)
O8	C37	1.342(2)	C6	C18	1.390(2)	C19	C20	1.393(2)	C36	C37	1.503(2)
O8	C38	1.439(2)	C7	C9	1.521(2)	C20	C21	1.519(2)			
C1	C2	1.401(2)	C8	C9	1.397(2)	C21	C23	1.521(2)			

Table SI 7: Bond Angles

			Angle/˚				Angle/˚				Angle/˚
C8	O2	C29	115.15(11)	C10	C9	C8	117.66(15)	C27	C22	C23	122.36(15)
C22	O4	C34	114.58(11)	C11	C10	C9	120.94(15)	C22	C23	C21	121.83(14)
C32	O6	C33	114.15(17)	C10	C11	C12	120.19(16)	C24	C23	C21	120.23(14)
C37	O8	C38	116.47(16)	C11	C12	C13	120.88(15)	C24	C23	C22	117.84(15)
O1	C1	C2	115.88(14)	C8	C13	C14	122.46(14)	C25	C24	C23	120.86(15)
O1	C1	C6	122.81(14)	C12	C13	C8	117.66(15)	C26	C25	C24	120.13(15)
C2	C1	C6	121.29(15)	C12	C13	C14	119.82(14)	C25	C26	C27	121.04(16)
C17	C1A	C19	119.64(16)	C13	C14	C16	111.82(13)	C22	C27	C26	117.58(15)
C1	C2	C28	120.04(15)	O3	C15	C16	115.96(14)	C22	C27	C28	122.59(14)
C3	C2	C1	118.58(16)	O3	C15	C20	122.61(14)	C26	C27	C28	119.80(15)
C3	C2	C28	121.37(15)	C20	C15	C16	121.42(14)	C2	C28	C27	111.82(13)
C4	C3	C2	120.92(16)	C15	C16	C14	120.19(14)	O2	C29	C30	106.69(13)
C18	C4	C3	119.65(17)	C17	C16	C14	121.52(14)	C29	C30	C5	112.64(15)
C32	C5	C30	113.75(16)	C17	C16	C15	118.24(15)	O5	C32	O6	122.98(18)
C1	C6	C7	121.12(15)	C1A	C17	C16	121.29(16)	O5	C32	C5	125.18(17)
C18	C6	C1	117.97(15)	C4	C18	C6	121.58(17)	O6	C32	C5	111.84(16)
C18	C6	C7	120.89(15)	C1A	C19	C20	121.32(16)	O4	C34	C35	107.66(13)
C6	C7	C9	111.93(13)	C15	C20	C21	121.45(14)	C34	C35	C36	114.30(14)
O2	C8	C9	118.25(14)	C19	C20	C15	118.08(15)	C37	C36	C35	111.58(14)
O2	C8	C13	119.09(14)	C19	C20	C21	120.46(14)	O7	C37	O8	122.97(16)
C9	C8	C13	122.51(15)	C20	C21	C23	111.75(13)	O7	C37	C36	125.66(17)
C8	C9	C7	121.93(15)	O4	C22	C23	118.17(14)	O8	C37	C36	111.37(15)
C10	C9	C7	120.26(15)	O4	C22	C27	119.37(14)				

Table SI 8: Hydrogen Atom Coordinates (Å×104) and Isotropic Displacement Parameters (Å2×103)

	x	y	z	U(eq)		x	y	z	U(eq)		x	y	z	U(eq)
H1	5137	3267	3554	40	H17	2138	-2136	1535	32	H33A	11123	871	1351	74
H3	5221	1881	1586	38	H18	1896	4540	5176	33	H33B	11743	1595	2329	74
H1A	1216	-1988	54	36	H19	2086	-349	-648	32	H33C	10884	2213	1622	74
H3A	2093	6349	3007	33	H21A	3846	1387	-721	26	H34A	6525	4993	924	27
H4	1090	5920	4315	36	H21B	5084	1807	83	26	H34B	6500	3765	265	27
H5A	8061	390	3321	36	H24	1618	2223	-595	27	H35A	8711	4274	1064	31
H5B	7249	1262	2815	36	H25	570	3836	-50	28	H35B	7954	3136	1445	31
H7A	3603	3305	5571	27	H26	1665	5231	1205	28	H36A	7478	4514	2730	33
H7B	4892	3281	5011	27	H28A	5151	5444	2299	28	H36B	9070	4429	2723	33
H10	1377	1803	4980	28	H28B	4060	6290	2087	28	H38A	7594	8077	2180	66
H11	371	-116	4223	30	H29A	6342	551	4505	29	H38B	8827	8290	2987	66
H12	1587	-1187	3228	28	H29B	6373	1824	5108	29	H38C	7283	8271	3210	66
H14A	4036	-1494	2831	26	H30A	8582	1816	4648	35					
H14B	5133	-305	2835	26	H30B	7890	2762	4145	35					

[1] a) Gutsche, C. D.; Muthukrishan, R. *Journal of Organic Chemistry* **1978**, *43*, 4905.

b) Gutsche, C. D.; Iqbal, M. *Organic Synthesis* **1990**, *68*, 234.

c) Gutsche, C. D.; Lin, L.-G. *Tetrahedron* **1986**, *42*, 1633.

d) Gutsche, C. D.; Levine, J. A.; Sujeeth, P. K. *Journal of Organic Chemistry.* **1985**, *50*, 5795.

[2] Frank, J. *Three-dimensional electron microscopy of macromolecular assemblies : visualization of biological molecules in their native state*; 2nd ed.; Oxford University Press: Oxford ; New York, 2006.

[3] Orlova, E. V.; Saibil, H. R. *Chemical Reviews* **2011**, *111*, 7710.

[4] van Heel, M.; Frank, J. *Ultramicroscopy* **1981**, *6*, 187.

[5] Case, D. A.; Darden, T. A.; T.E. Cheatham, I.; Simmerling, C. L.; Wang, J.; Duke, R. E.; Luo, R.; Walker, R. C.; Zhang, W.; Merz, K. M.; Roberts, B.; Hayik, S.; Roitberg, A.; Seabra, G.; Swails, J.; Götz, A. W.; Kolossváry, I.; Wong, K. F.; Paesani, F.; Vanicek, J.; Wolf, R. M.; Liu, J.; Wu, X.; Brozell, S. R.; Steinbrecher, T.; Gohlke, H.; Cai, Q.; Ye, X.; Wang, J.; Hsieh, M.-J.; Cui, G.; Roe, D. R.; Mathews, D. H.; Seetin, M. G.; Salomon-Ferrer, R.; Sagui, C.; Babin, V.; Luchko, T.; Gusarov, S.; Kovalenko, A.; Kollman, P. A.; University of California, San Francisco: 2012.

[6] Wang, J. M.; Wolf, R. M.; Caldwell, J. W.; Kollman, P. A.; Case, D. A. *Journal of Computational Chemistry* **2004**, *25*, 1157.

[7] Joung, I. S.; Cheatham, T. E. *Journal of Physical Chemistry B* **2008**, *112*, 9020.

[8] Bayly, C. I.; Cieplak, P.; Cornell, W. D.; Kollman, P. A. *Journal of Physical Chemistry* **1993**, *97*, 10269.

[9] Gaussian 09, Revision D.01, Frisch, M. J.; Trucks, G. W.; Schlegel, H. B.; Scuseria, G. E.; Robb, M. A.; Cheeseman, J. R.; Scalmani, G.; Barone, V.; Mennucci, B.; Petersson, G. A.; Nakatsuji, H.; Caricato, M.; Li, X.; Hratchian, H. P.; Izmaylov, A. F.; Bloino, J.; Zheng, G.; Sonnenberg, J. L.; Hada, M.; Ehara, M.; Toyota, K.; Fukuda, R.; Hasegawa, J.; Ishida, M.; Nakajima, T.; Honda, Y.; Kitao, O.; Nakai, H.; Vreven, T.; Montgomery, J. A., Jr.; Peralta, J. E.; Ogliaro, F.; Bearpark, M.; Heyd, J. J.; Brothers, E.; Kudin, K. N.; Staroverov, V. N.; Kobayashi, R.; Normand, J.; Raghavachari, K.; Rendell, A.; Burant, J. C.; Iyengar, S. S.; Tomasi, J.; Cossi, M.; Rega, N.; Millam, M. J.; Klene, M.; Knox, J. E.; Cross, J. B.; Bakken, V.; Adamo, C.; Jaramillo, J.; Gomperts, R.; Stratmann, R. E.; Yazyev, O.; Austin, A. J.; Cammi, R.; Pomelli, C.; Ochterski, J. W.; Martin, R. L.; Morokuma, K.; Zakrzewski, V. G.; Voth, G. A.; Salvador, P.; Dannenberg, J. J.; Dapprich, S.; Daniels, A. D.; Farkas, Ö.; Foresman, J. B.; Ortiz, J. V.; Cioslowski, J.; Fox, D. J. Gaussian, Inc., Wallingford CT, 2009

[10] Darden, T.; York, D.; Pedersen, L. *Journal of Chemical Physics* **1993**, *98*, 10089.

[11] Berendsen, H. J. C.; Grigera, J. R.; Straatsma, T. P. *Journal of Physical Chemistry* **1987**, *91*, 6269.

[12] (a) Kumar, S.; Bouzida, D.; Swendsen, R. H.; Kollman, P. A.; Rosenberg, J. M. *Journal of Computational Chemistry* **1992**, *13*, 1011.

(b) Grossfield, A; code available at http://membrane.urmc.rochester.edu/